CODE_BRIGHT

A 3-D program for thermo-hydro-mechanical analysis in geological media

5th WORKSHOP OF CODE_BRIGHT USERS

Barcelona, 7th May 2013

Department of Geotechnical Engineering and Geosciences

(UPC, Barcelona, Spain)

CIMNE

(Centro Internacional de Métodos Numéricos en Ingeniería, Barcelona, Spain)

CONTENTS

THM MODELLING OF ONKALO PROJECT

Erdem Toprak*, Sebastia Olivella†

Department of Geotechnical Engineering and Geosciences Technical University of Catalonia (UPC) Campus Norte UPC, 08034 Barcelona, Spain

Key words: THM coupled analysis, gap modeling, buffer-backfill interface

Abstract: *This paper is concerned with preliminary analyses of coupled Thermo-Hydro-Mechanical (THM) processes in the ONKALO Project. It is a project of Finland and it will be the final disposal repository of nuclear waste. The Code_Bright finite-element software program is used in performing the modelling and calculations. The objective of the study was to analyse important design parameters of the project such as the time required for reaching full saturation, maximum temperature reached in canister, deformations in the buffer-backfill interface and also modeling of gap between canister and buffer.*

1. INTRODUCTION

The ONKALO will be a part of the final repository, which will consist of tunnels excavated at a depth of approximately 460 m and located at approximately 25 m from each other. The spent fuel will be encapsulated in final disposal canisters made of cast iron, enclosed in a copper shell. These canisters will be placed in holes drilled at the bottom of the repository tunnels and surrounded with bentonite clay. Figure 1.1 shows a possible design of disposal facility.

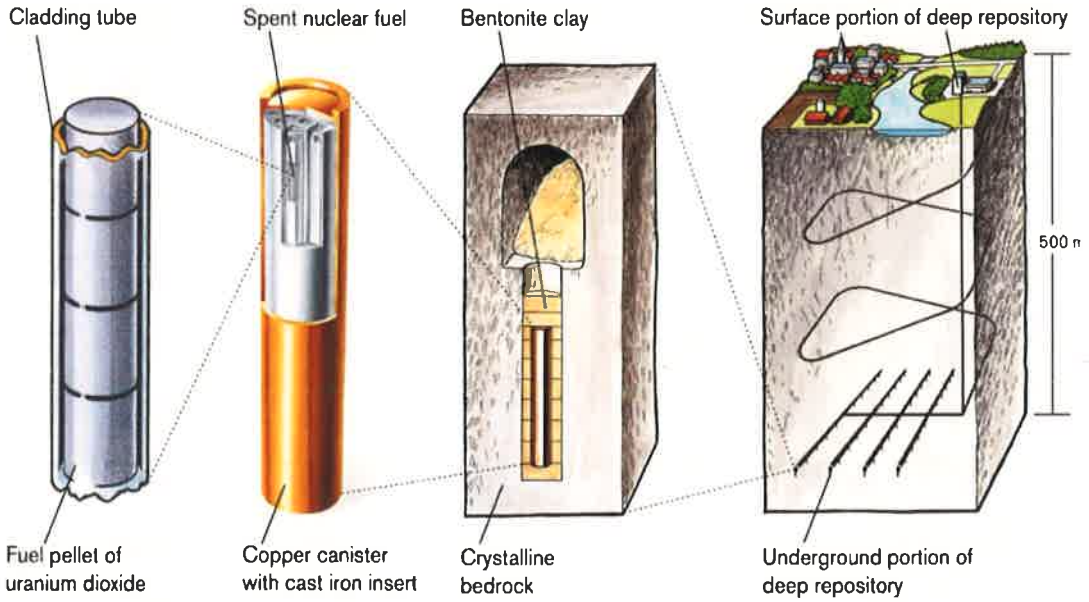

Figure 1.1: A possible design of the final disposal facility planned to be constructed at the Olkiluoto site

Regarding to THM analysis, a fundamental issue was to determine relevant thermal boundary conditions. The main reason is that it is not possible to extend boundaries at the distance the thermal problem would require because the THM problem should be

solved in a relatively limited domain so the details are well captured. As indicated by Ikonen (2005), the maximum permitted canister temperature is set to 90°C. This essential functional requirement for deposition tunnel is a main part of thermal modeling task.

With regard to the hydraulic analyses, the time required for full saturation is sensitive to vapor diffusion or heat transport, intrinsic permeability and suction relation. It has been undertaken a sensitivity study to observe the base case performance and its correspondence with realistic conditions.

There is an air-filled gap between canister and the buffer ring. In its unsaturated state, buffer will not transfer heat efficiently that may disturb the heat dissipation and lead to higher canister temperature. Therefore gap modeling was an essential part of this study.

The modeling process of buffer-backfill interface is an important part of tunnel backfill design. The calculations will aim to find out deformations in this interface. A series of laboratory tests have been started up by POSIVA in order to investigate the hydro-mechanical behavior of MX80 bentonite. The BBM parameters of buffer and backfill, obtained from laboratory tests, are shown in the Table 1.

Parameters	Symbols	Units	Buffer (MX80)	Backfill (Friedland-clay)
Parameters for elastic compressibility against mean stress change	κ_{i0}	-	0.05	0.05
	α_i	-	-0.003	-0.003
Parameters for elastic volumetric compressibility against suction change	κ_{s0}	-	0.25	0.025
	α_{sp}	-	-0.145	-0.145
	p_{ref}	MPa	0.01	0.01
Elasto-plastic volumetric compressibility	$\lambda(0)$	-	0.15	0.3
Parameters to define LC yield curve	r	MPa^{-1}	0.8	0.8
	β		0.02	0.02
Reference stress	p^c	MPa	0.01	0.01
Slope of critical state	M	-	1.07	1.07
Parameter for the plastic potential	α	-	0.53	0.53
Initial pre-consolidation stress for saturated conditions	po^*	MPa	12	0.5

Table 1 BBM parameters used for the buffer and backfill

2. RESULTS

Maximum temperature, time needed to full saturation of bentonite buffer, swelling pressure of bentonite buffer and displacements occurred at the interface of buffer and backfill are the main interest of this study. The most important results obtained for buffer material are summarized in Table 2 beside this Figure 2.1 shows the evolution of the temperature, liquid pressure, porosity and vertical displacements in the buffer, backfill and pellets at the end of the 30 years.

Analyzed parameters	Reached values
Maximum temperature in buffer	~ 82 °C
Time to reach full saturation of buffer	~ 50 years
Achieved maximum suction in buffer	85 MPa
Dry density of buffer	1700-1750 kg/m^3
Swelling pressure of buffer	6-9 MPa
Displacements at the interface of buffer-backfill	10 -16 cm

Table 2 Evolution of important parameters for buffer

In the first phase of the study thermal calculations have been carried out in order to set up appropriate thermal boundary conditions. Secondly, laboratory tests were modeled in order to determine the BBM parameters of buffer and backfill. Finally, THM calculations were performed considering different effects and geometries (for example air gap between canister and buffer).

THM response of backfill, pellet, rock and air-gap has been presented in the study. However, laboratory tests for these materials have been going on and therefore a further study is to be to be performed to validate BBM parameters used for these materials.

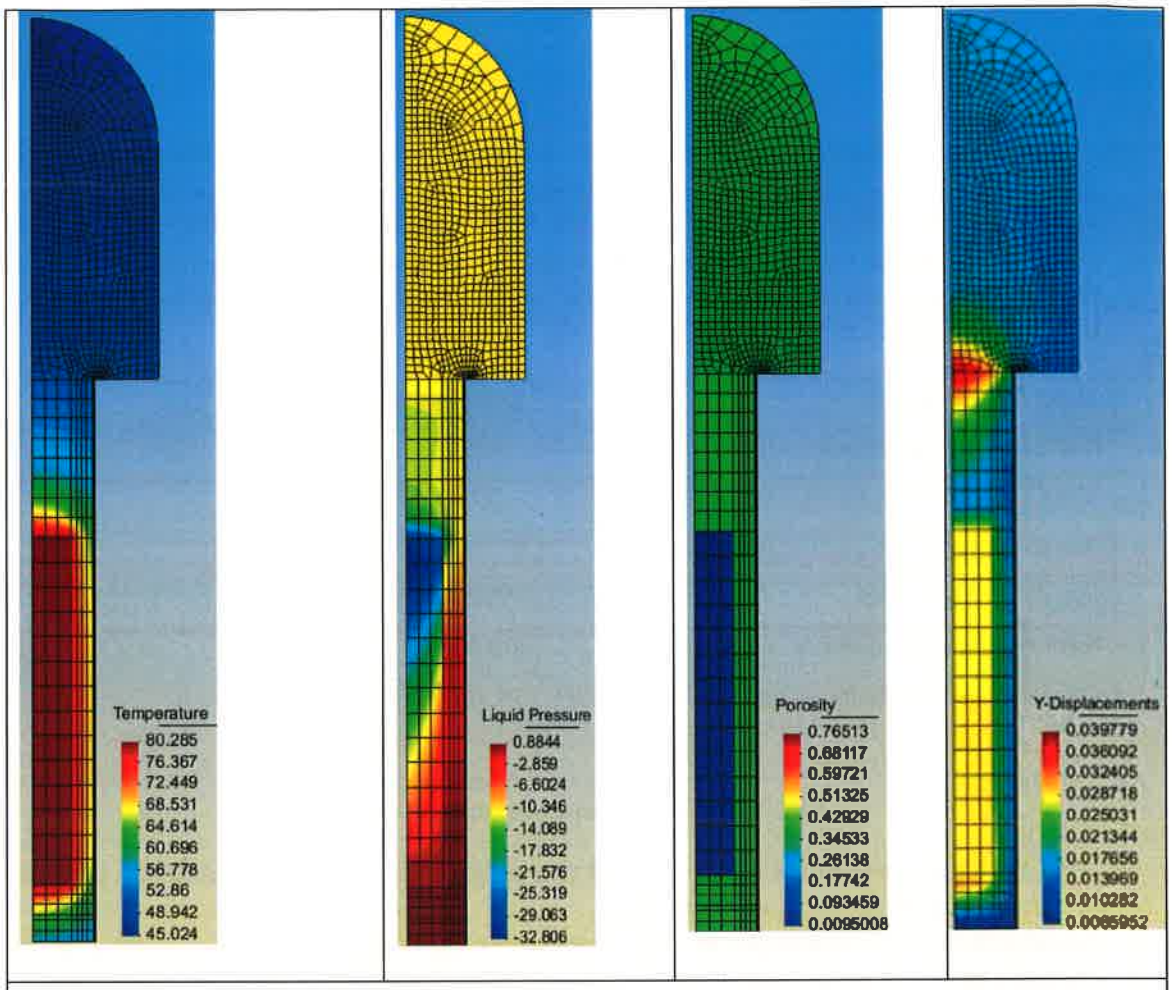

Figure 2.1: Evolution of temperature, liquid pressure, porosity and vertical displacement (30 years)

References

Alonso E.E., Gens A and Josa A, 1990."A constitutive model for partially saturated soils". Géotechnique, 40(3): 405-430

Hokmark. Harald. October 2003. Hydration of the bentonite buffer in a KBS-3 repository. Clay Technology AB, Ideon Research Centre, 223 70 Lund, Sweden

Ikonen, Kari. June 2003. Thermal Analyses of Spent Nuclear Fuel Repository

Toprak Erdem, Nadia Mokni, Sebastia Olivella, November 2011. Thm Modelling of Onkalo Project Preliminary Modelling Study.

3-D THERMO-HYDRAULIC MODELLING OF DEMONSTRATION TESTS IN A SPENT NUCLEAR FUEL REPOSITORY

Pintado X. and Rautioaho E.

B+TECH Oy, Laulukuja 4, FI-00420, Helsinki, Finland
e-mail: xavier.pintado@btech.fi

Key words: Spent fuel repository, demonstration test, fracture

Abstract. *In the reference design for the spent nuclear fuel repository in Finland, the metal canisters filled with the spent fuel are surrounded by a protective layer of bentonite blocks. Posiva is planning to initiate some demonstration tests to simulate this concept. The plans include the heating of the canister and the instrumentation of the EBS (Engineer Barrier System) and the rock. In order to estimate the tendency of the saturation process and the temperature distribution, a 3-D thermo-hydraulic analysis has been conducted using the demonstration test geometry.*

1 INTRODUCTION

The bentonite blocks which constitute the EBS surrounding the canisters hydrate with the groundwater flow. The rock hosting the repository is crystalline and fractured. The water flows mainly through the fractures, which have a wide range of sizes.

The process of modelling the fractured rock system with finite element codes is not evident, as the codes run well for continuous media but discrete media, such as fractured rock, present some drawbacks which should be dealt with.

The main problem is to simulate the presence of fractures. First, the fractures need to be identified with a geological mapping. Secondly, the properties of the fractures have to be measured with "in situ" tests. The rock between the identified fractures is often fractured as well with smaller fractures that could not be identified during the mapping.

Groundwater flow in fractured media is simulated by assuming the fractures are planes in the rock mass. Depending on the capabilities of the code used for the simulation, the either all of the fractures or only a small part of them can be directly simulated. The problem addressed in this work has been simulated with CODE_BRIGHT [1] and fractures are implemented using volumetric elements. Three different cases are presented: Case 1 contains no fracture, and Case 2 and Case 3 contain a single fracture. The difference between Case 2 and Case 3 is in the intrinsic permeability employed in the rock.

2 MODEL DESCRIPTION

2.1 Geometry

The geometry consists of a cuboid with a length of 188 m, a width of 126 m and a height of 58.9 m. The deposition holes are 7.8 m deep and 1.75 m in diameter, and the canister is 4.8 m long and 1.05 m in diameter (Figure 1). A fracture intersecting the deposition holes has

been simulated in two of the cases. The thickness of the fracture is 0.2 m (Figure 2). The finite element mesh has 62 344 nodes and 294 625 elements when the fracture is not incorporated, and 115 705 nodes and 597 515 elements when the fracture is present.

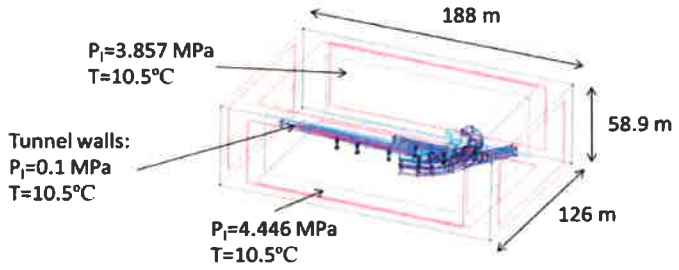

Figure 1. Dimensions of the cuboid geometry and the fixed boundary conditions. The fracture is not present in this geometry.

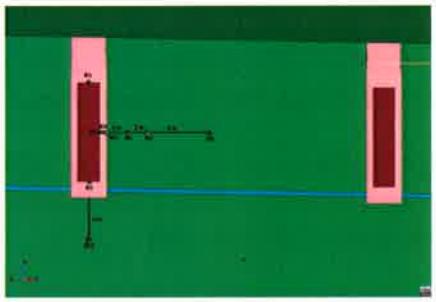

Figure 2. Deposition holes, fracture and calculation points.

2.2 Material parameters

As a thermo-hydraulic analysis was performed, the required parameters are the porosity, the intrinsic permeability, the water retention curve parameters following the van Genuchten model [2], the specific heat and the thermal conductivity (Table 1). For the bentonite buffer, a tortuosity factor of 0.4 has been selected and in the Brooks and Corey [3] law for relative permeability an exponent of 3 has been employed.

2.3 Boundary conditions

The excavated tunnels and deposition holes have a boundary condition of atmospheric liquid pressure and constant temperature before canister and buffer installation.

The canister boundary condition is a constant temperature of 90°C and zero flow is assumed on the top boundary of the buffer.

The boundary conditions on the vertical planes of the cuboid geometry are no-flow conditions. The top and bottom planes have a constant hydrostatic liquid pressure and a constant temperature (Figure 1).

Table 1. Material properties

	Porosity	Intrinsic permeability (m^2)	P_0 (MPa)	λ	Specific heat (J/kgK)	Thermal conductivity (W/mK)
Rock	0.02	$1.52x10^{-19}$ / $1.52x10^{-24}$ (*)	1.5	0.3	784	2.61
Fracture	0.02	$5.0x10^{-15}$	1.5	0.3	784	2.61
Buffer	0.438	$5.59x10^{-21}$	31.25	0.5	800	0.3/1.3(**)

(*) Intrinsic permeability for Case 1 and Case 2 / Case 3
(**) Dry/saturated

3 SIMULATION RESULTS

The evolution of the degree of saturation and temperature has been analyzed.

3.1 Degree of saturation evolution

The effect of the fracture is clear in all cases. Case 1 and Case 2 have similar evolution and the influence of the fracture is not important. In Case 3, there is a clear difference in results when the calculation point is near the fracture (the bottom of the canister, Figure 4) and when the calculation point is far from the fracture (the top of the canister, Figure 3), as is expected.

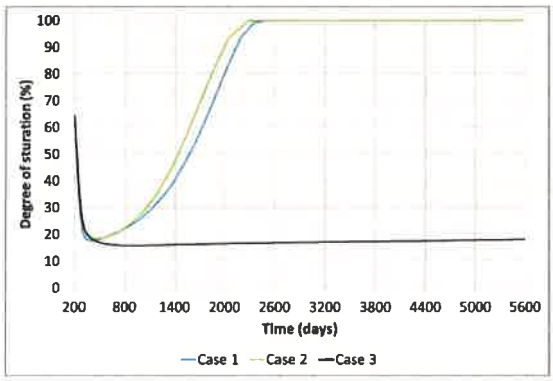

Figure 3. Evolution of degree of saturation at the top of the canister.

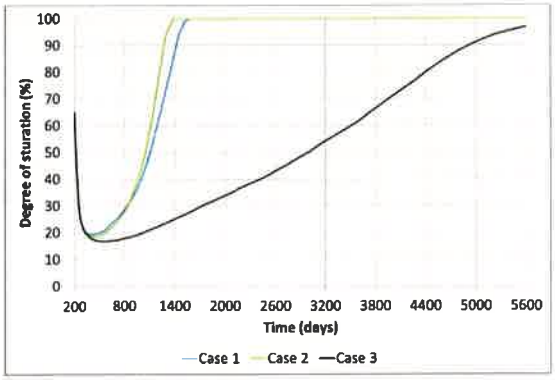

Figure 4. Evolution of degree of saturation at the bottom of the canister.

3.2 Temperature evolution

The temperature evolution in the rock has been analyzed (Figures 5 and 6). A clear difference can be seen in the results when the rock has low hydraulic conductivity: The boundary condition in the canister is a constant temperature and the buffer transports less heat

when it is dry (lower thermal conductivity), so less heat arrives to the rock and the temperature does not increase as quickly as it would if the buffer had higher thermal conductivity.

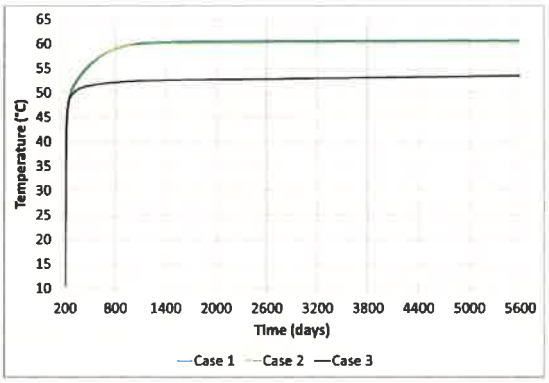

Figure 5: Temperature evolution on the buffer-rock interface at canister mid-height.

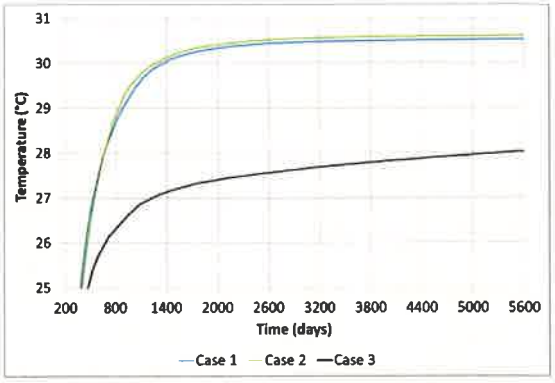

Figure 6: Temperature evolution in the rock 2 m from the deposition hole wall at canister mid-height.

4 CONCLUSIONS

- The saturation process could be fairly independent of the presence of fractures if the rock mass had a sufficiently high hydraulic conductivity (> 10^{-19} m^2).
- The fracture location is important to the buffer saturation process when the rock mass has low hydraulic conductivity.
- The boundary conditions on the outer boundaries of the model should be fixed sufficiently far from the test area and they should evolve with time. The task of determining the boundary conditions and their location could be conducted with regional groundwater flow models for the hydraulic boundary condition (Löfman [4]) and with thermal analytical solutions for thermal boundary condition (Ikonen [5])
- The mapping and evaluation of the fracture properties is important for the correct interpretation of the demonstration test with regard to the development of saturation and temperature at the test site.
- The implementation of 2-D fracture planes could increase the number of fractures that can be incorporated into the model and improve the computation time.

REFERENCES

[1] Olivella, S., J. Carrera, A. Gens, E. E. Alonso, 1994a. Non-isothermal Multiphase Flow of Brine and Gas through Saline media. Transport in Porous Media, 15, 271:293

[2] van Genuchten, R., 1980. A closed-form equation for predicting the hydraulic conductivity of unsaturated soils. Soil Science Society American Journal, 44: 892-898

[3] Brooks, R.H., Corey, A.T., 1964. Hydraulic Properties of Porous Media. Hydrologic Paper 3, Colorado State University, Fort Collins, USA

[4] Löfman, J., Poteri, A., Pitkänen, P., 2010. Modelling of Salt Water Upconing in Olkiluoto. Posiva Working report 2010-25. Eurajoki, Finland

[5] Ikonen, K., 2009. Thermal dimensioning of spent fuel repository. Posiva Working report 2009-69. Eurajoki, Finlan

VIRTUAL UNDERGROUND LABORATORY FOR ROCK SALT - VIRTUS

K. Wieczorek and O. Czaikowski

Gesellschaft für Anlagen und Reaktorsicherheit (GRS)
Theodor-Heuss-Strasse 4, 38122 Braunschweig, Germany
e-mail: oliver.czaikowski@grs.de, web page: http://www.grs.de

Key words: Nuclear waste disposal, underground laboratory, process visualisation

Abstract. *With respect to disposal in rock salt, a virtual underground laboratory (VIRTUS) is developed by GRS, BGR, DBE TEC and the contractor IFF. VIRTUS combines powerful visualisation software for geologic models and result data of numerical simulations with functions for management of material and project data. In that, VIRTUS is a software platform and data swivel at the same time. Geologic models are imported into VIRTUS, powerful edit functions allow the creation of mine structures which are integrated into the geology, the resulting models or details of them can be exported to process-level codes (here CODE_BRIGHT), where they are used as input for model calculations on the coupled thermal-hydraulic-mechanical behaviour of the system consisting of waste, technical components and rock formation.*

1 INTRODUCTION

In the last decade the safety concept in Germany for the final disposal of HLW in rock salt has been refined. In the past, conservative release scenarios were considered. Now the concept focuses on the systematic demonstration of the long-term safe containment of the radioactive waste by demonstrating the long-term effectiveness and integrity of the geological and geotechnical barriers, BMU 2010 report[i].

With respect to the international experience gained in the field of geological radioactive waste disposal, it is widely agreed that the overall detection of the geo-hydro-mechanical conditions and their changes due to thermal disturbances via in-situ measurements is one of the most relevant prerequisites for sound understanding of host rock behaviour. An adequate understanding of related coupled processes is needed for the development of reliable physical models needed for numerical simulation repository performance. Several international Underground Rock Laboratories (URL's) are run under this scope of work in soft clays, indurated clays and in crystalline rock.

2 METHODOLOGY

Recently, there has been no saliniferous formation open to the international scientific experience which could provide measurements in-situ. With respect to disposal in rock salt, GRS therefore develops the virtual underground laboratory (VIRTUS) in co-operation with the Bundesanstalt für Geowissenschaften und Rohstoffe (BGR) and the DBE Technology GmbH (DBE TEC) with the contractor Fraunhofer Institut für Fabrikbetrieb und –automatisierung (IFF).

VIRTUS combines powerful visualisation software for geologic models and result data of numerical simulations with functions for management of material and project data. In that, VIRTUS is a software platform and data swivel at the same time. Geologic models are

imported into VIRTUS, powerful edit functions allow the creation of mine structures which are integrated into the geology, the resulting models or details of them can be exported to process-level codes (usually finite element codes), where they are used as input for model calculations on the coupled thermal-hydraulic-mechanical behaviour of the system consisting of waste, technical components and rock formation.

The process-level code GRS is using with VIRTUS is the computer code CODE_BRIGHT developed by UPC, used for 2D and 3D analysis of coupled hydro-mechanical (THM) phenomena in geological media. The development of CODE_BRIGHT started in the 1990's with the purpose of modelling the response of saline materials in the context of underground nuclear waste disposal. Details about the basic theories with the formulated governing equations (balance equations, constitutive models and equilibrium relationships) are described in the code manual[ii].

The simulation results from CODE-BRIGHT can be imported and visualised in VIRTUS in context with the underlying geology. The service-oriented structure of VIRTUS allows access via internet as well as working on a local platform.

The material data required for the simulations are stored in the VIRTUS database. An important part of the project is the collection and evaluation of existing data on the rock and the technical components.

In the current project stage, a prototype of VIRTUS is existing and is continuously extended[iii]. At present, three virtual experiments of different complexity are defined, which are modelled in the frame of the current project phase. With them, the complete workflow given below will be demonstrated:

- Import of the geologic model
- Generation of the mine structure and integration in the geology
- Export of different model parts to the process-level codes (PLC)
- Finite element mesh generation and simulation calculation by the PLC (outside VIRTUS)
- Import and visualization of the simulation results in VIRTUS

3 ACKNOWLEDGEMENTS

The authors gratefully acknowledge the funding by the German Ministry of Economics and Technology (BMWi) under contract no. 02 E 10890.

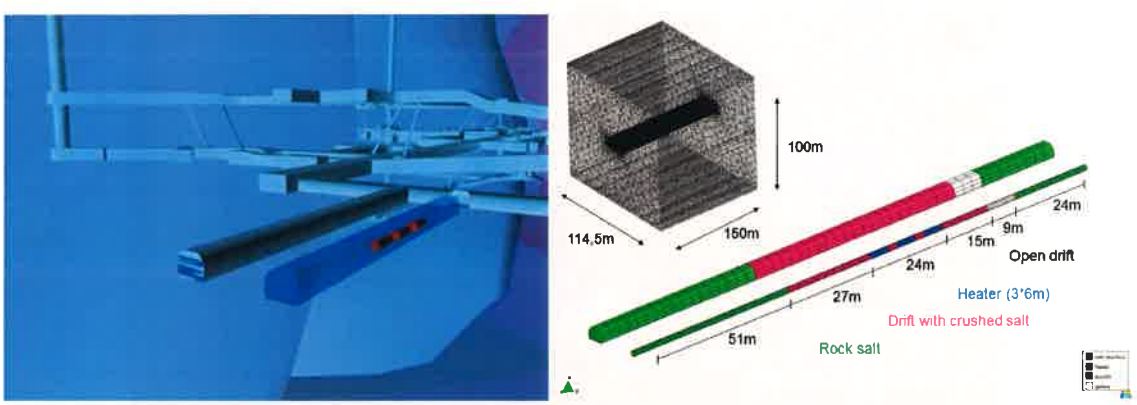

Figure 1(a): 3D geometry of a virtual mine structure – existing mine structures can be imported and new structures can be generated and edited within VIRTUS (*left*) and FE model geometry used for CODE_BRIGHT calculation (*right*)

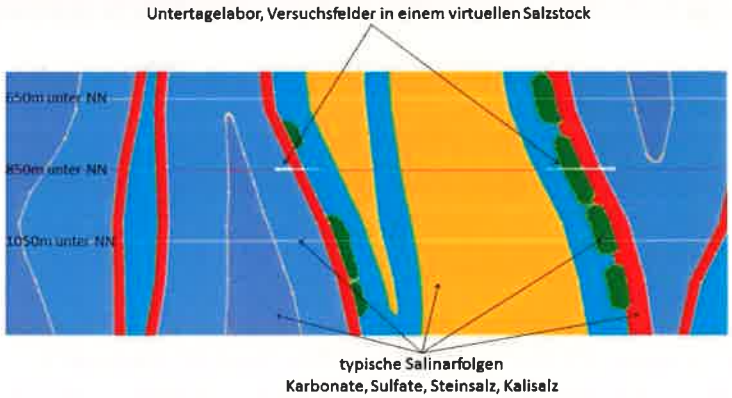

Figure 1(b): Vertical section of a virtual salt dome with typical saline series

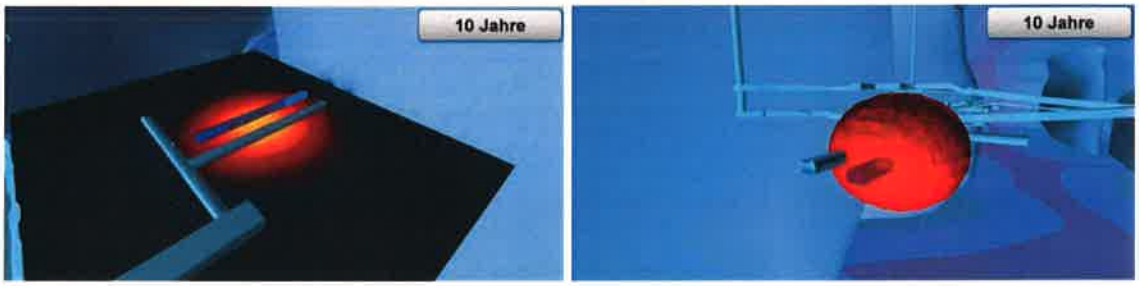

Figure 1(c): Visualisation of the temperature field around two drifts heated by POLLUX casks (*left*: horizontal section, *right*: 3D evolution)

Figure 1(d): Virtual model of an underground laboratory in 360-degree representation at the Fraunenhofer IFF.

REFERENCES

[i] BMU 2010. Bundesministerium für Umwelt, Naturschutz und Reaktorsicherheit: Sicherheitsanforderungen an die Endlagerung wärmeentwickelnder radioaktiver Abfälle. Stand 30. September 2010

[ii] CODE_BRIGHT, 2002. A 3D program for thermo-hydro-mechanical analysis in geological media. Users guide

[iii] Rothfuchs, T., S. Masik, J. Behlau, M. Jobmann, 2012: Projekt VIRTUS – Virtuelles Untertagelabor im Salz. 9. Fachtagung „Digitales Engineering zum planen, testen und betreiben technischer Systeme", 15. IFF-Wissenschaftstage 26. – 28. Juni 2012, pp 285-292.

FINITE ELEMENT ANALYSIS OF COUPLED PHENOMENA INDUCED IN A GRANULAR MATERIAL BY FREEZING AND THAWING

Francesca Casini*, Antonio Gens*, Sebastia Olivella*, Giulia Viggiani°

* Department of Geotechnical Engineering and GeosciencesTechnical University of Catalonia (UPC) Campus Norte UPC, 08034 Barcelona, Spain
Email: francesca.casini@upc.edu; antonio.gens@upc.edu; sebastia.olivella@upc.edu

° *DICII, Università di Roma* Tor Vergata, *Roma, Italy*
Email: viggiani@uniroma2.it

Keywords: Artificial ground freezing, Coupling, Ice Retention Model,

Abstact. *Freezing and thawing of pore fluid within soils involves complex thermal, hydraulic and mechanical processes that can have significant mutual geotechnical interactions. For example, phase changes of pore fluid caused by temperature variations modify the hydraulic regime of the soil, which in turn induces mechanical deformation. At the same time, any change in the hydraulic and mechanical conditions influences the thermal processes by advection and changes of ice and water contents.*
One of the techniques involving freezing and thawing of granular material is Artificial Ground Freezing (AGF). This is a controllable process that can be used in civil engineering to stabilise temporarily the ground, provide structural support, and/or exclude groundwater from an excavation until construction of the final lining provides permanent stability and water tightness. AGF is often carried out based on an observational approach, while a full understanding of the freezing process and of the generation of freezing-induced heave and settlements is still far from being achieved.
This work investigates the heave and settlement induced by freezing and thawing of the soil; the final objective of the work is to develop a tool to obtain reliable and effective predictions of ground displacements induced by AGF. A constitutive model that encompasses frozen and unfrozen behaviour within an unified effective-stress based framework was adopted; this employs a combination of ice pressure, liquid pressure and total stress as state variables.
The performance of the model was evaluated simulating the behaviour a disc of soil elements in axial symmetric conditions, using a linear elastic constitutive model and the Bishop stress extended to frozen conditions for the mechanical part (M). The frozen/unfrozen water content was evaluated with an Ice Retention Model that links the suction, defined as the difference of ice and pore water pressure, to the degree of saturation of unfrozen water with a van Genuchten function (H). The conductive heat flux was evaluated using the Fourier law and the overall thermal conductivity was calculated as the geometric mean of the soil mass consisting of soil minerals and pore water or ice (T). The results of two numerical simulations with different Young's Modulus are compared in order to have a better understanding of the influence of the soil stiffness on the evolution of ground displacements during freezing and thawing.

1 ADOPTED THERMO-HYDRO-MECHANICAL MODEL

The adopted constitutive model was originally developed by [1]Nishimura *et al.* (2009) extending a THM model developed by [2,3,4] for high temperature problems and replacing the gas phase by solid ice phase. The performance of the constitutive model, which has been implemented in CODE_BRIGHT, was evaluated through the simulation of a disc... of elements in axial symmetric conditions subjected to freezing and thawing (for the details of the constitutive model see [1,5, 6]).

1.1 Geometry, initial and boundary conditions

The model consists of a disc of height H=1m and radius R=30 m (see Figure 1) in Figure 1. The total simulation time is equal to 39999 days, subdivided in five phases, as detailed below:

1) Consolidation: t=0-1 day, T_0=15° C, p_{w0}=0 kPa, n_0=0.5 σ_{v0}=σ_{h0}=200 kPa;
2) Freezing at the centre boundary: t=1-20 days, T=15-65° C;
3) maintenance of constant temperature at centre boundary: t=20-20000 days, T=-50°C;
4) Thawing at centre boundary t=20000-20019 days, T=-50+65° C;
5) maintenance at boundary T=15°C t=20019-39999 days.

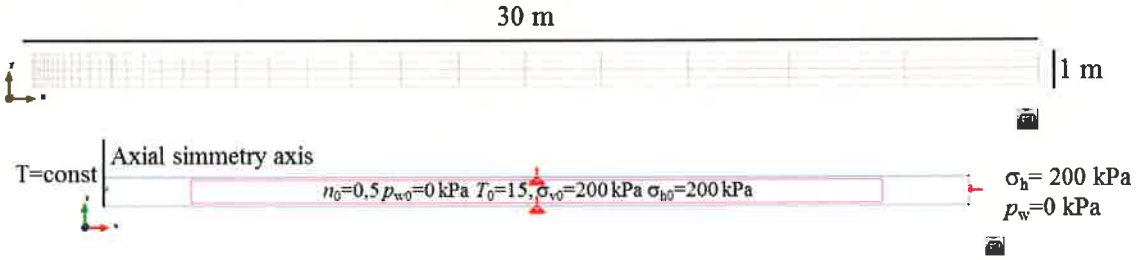

Figure 1. Geometry, mesh and initial conditions

1.2 Model parameters

The material was modelled as linear elastic with ν=0.3 and Young's Modulus E_1=100 MPa and E_2=1000 MPa respectively. The Ice Retention Model and the liquid phase relative permeability were represented using a Van Genuchten model [7] with parameters characteristic of volcanic ash soils: ice entry value, P = 10 kPa, exponent λ = 0.25, S_{lsat}=1 and S_{lres}=0, and an intrinsic permeability K=1e^{-13} m^2. The thermal conductivity of the soil minerals and pore materials was computed as the geometric mean using he following equations: $\lambda = \lambda_{unfrozen}^{S_l}\lambda_{frozen}^{(1-S_l)}$; $\lambda_{unfrozen} = \lambda_{solid}^{(1-n)}\lambda_{water}^{n}$; $\lambda_{frozen} = \lambda_{solid}^{(1-n)}\lambda_{ice}^{n}$, with λ_{ice}=2.2 W/mK, λ_{water}=0.57 W/mK and λ_{solid}=0.14 W/mK (after [8]).

2 NUMERICAL RESULTS

The profiles of the temperature at the end of the main phases are shown in Figure 2. At the end of the freezing phase (20 days) the temperature below zero is extended up to 0.2 m form the centre; after 20000 days the below zero area reaches up to 7.2 m from the centre. At the end of the thawing phase (20019 days) the temperature profile changes only for x≤1.8m, at t=39999 days the temperature is increasing for x≤12.8m, while a decrease of temperature is predicted for x>12.8 m.

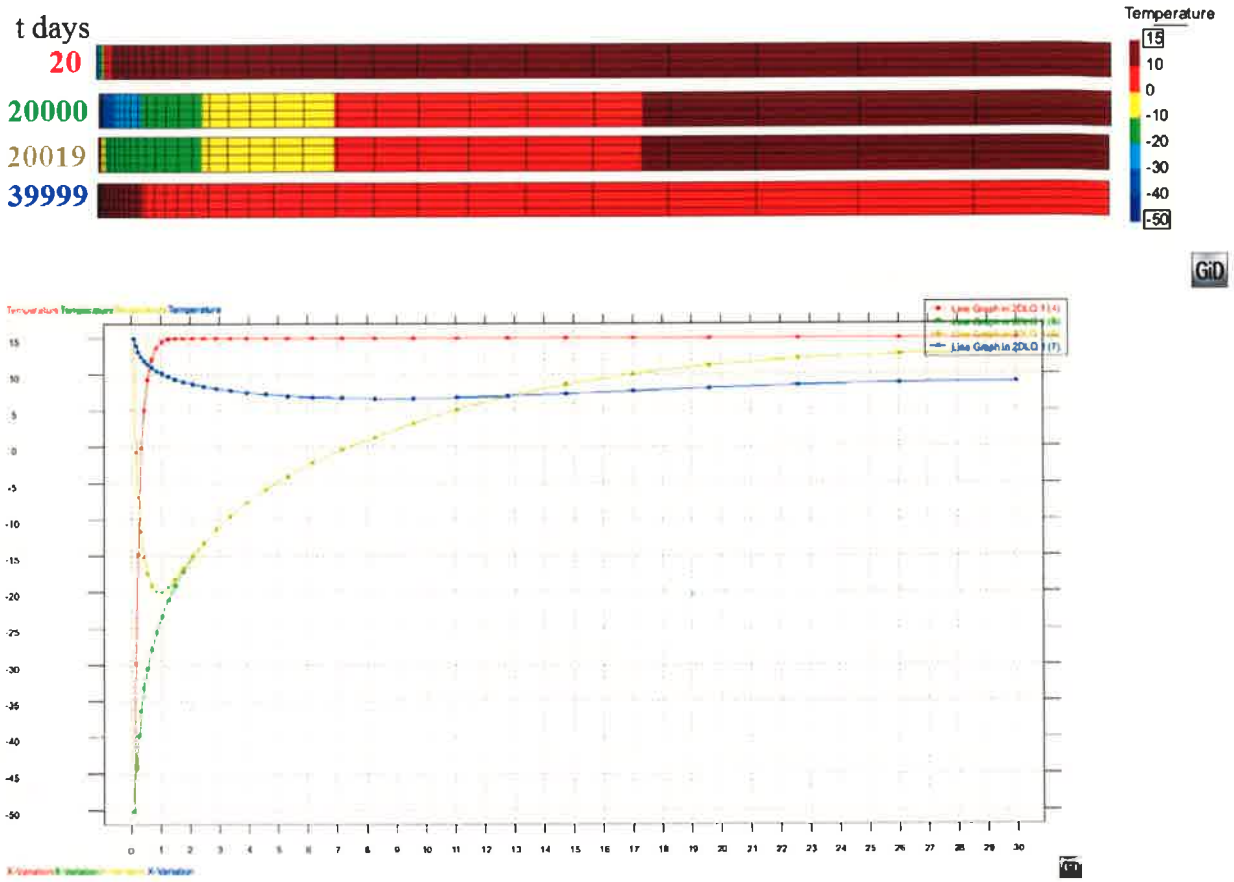

Figure 2 Contour fill and temperature profiles at the end of each phase.

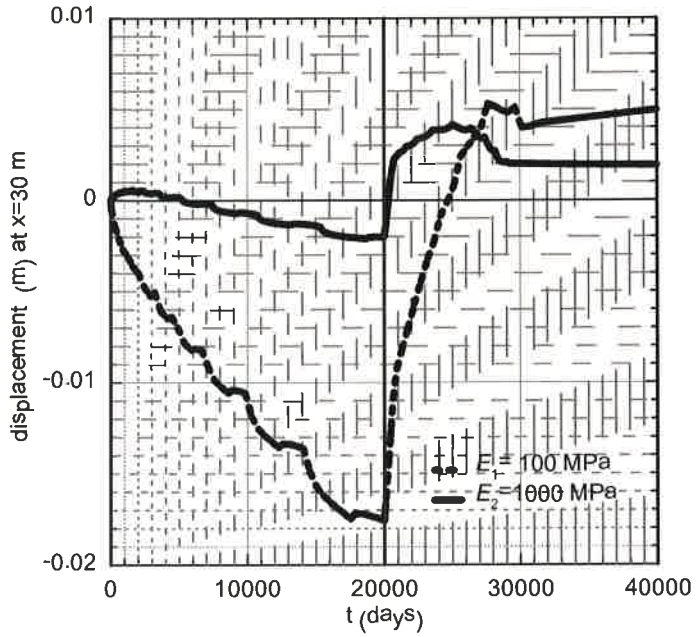

Figure 3. Comparison of displacement evolution with time in the x direction at x=30 m.

Figure 3 shows the results obtained from the two numerical simulations carried out using different stiffness. During the freezing phase, the stiffer material (E_2) first contracts up to ~0.8 mm at the far border, while at the end of freezing it swells to -2 mm

(t=20000 days), while, the softer material (E_1) only experiences swelling of about -17.5 mm. During the thawing phase, both models experienced contraction at the far border with a peak of 4 mm and a drop to a quasi-constant value of 2 mm for the stiffer material. The softer material shows a peak of 5 mm, which is delayed in time, followed by a slight drop and a linear increase with time. This different behaviour in term of cumulative displacements at the far border is probably due be due to the different stress paths followed during freezing and thawing.

CONCLUSIONS

A disc of a sandy materials subject to freezing and thawing was modelled with a THM elastic linear model implemented in CODE_BRIGHT. Two numerical simulation were carried out performed with different values of stiffness. The softer material shows one order of magnitude higher cumulative displacements at the far border during freezing and a 2.5 time contraction with a slower response during thawing, compared to the stiffer material. Further investigations are required on the stress paths followed by the ground at different distances from the freezing/thawing source using an elasto-plastic constitutive model.

[1] Nishimura, S., Gens, A., Olivella, S. & Jardine, R.J. (2009). THM-coupled finite element analysis of frozen soil: formu-lation and application. Géotechnique 59(3): 159-171.

[2] Olivella, S., Carrera, J., Gens, A. & Alonso, E. E. (1994). Non-isothermal multiphase flow of brine and gas through saline media. Transp. Porous Media 15(3): 271–293.

[3] Olivella, S., Gens, A., Carrera, J. & Alonso, E. E. (1996). Nu-merical formulation for a simulator 'CODE_BRIGHT' for thecoupled analysis of saline media. Engng Comput. 13(7): 87–112.

[4] Gens, A., Garcia-Molina, A. J., Olivella, S., Alonso, E. E. & Huertas, F. (1998). Analysis of a full scale in situ test simu-lating repository conditions. Int. J. Numer. Anal. Methods Geomech. 22(7): 515–548.

[5] Gens, A. (2010). Soil-enviroment interactions in geotechnical engineering. Géotechnique 60(1): 3-74.

[6] Casini, F., Gens, A., Olivella, S. Viggiani, G.M.B. (2013). Coupled phenomena induced by freezing in a granular material. Coupled Phenomena in Enviromental Geotechnics (CPEG), 1-3 July 2013, Torino, Italy.

[7] van Genuchten, M. Th. (1980). A closed-form equation for predicting the hydraulic conductivity of unsaturated soils. Soil Sci. Soc. Am. J. 44: 892–898.

[8] Papakonstantinou, S., Anagnostou, G. & Pimentel, E. (2012). Evaluation of ground freezing data from the Naples sub-way. Proceedings of the ICE: Geotechnical Engineering. DOI: 10.1680/geng.10.00099

HYDRIC CHANGES IN A ROAD EMBANKMENT UNDER CLIMATIC ACTIONS

Garcia E., Vaunat J. and Villarraga C.

Department of Geotechnical Engineering and Geosciences, UPC, Barcelona, Spain

Abstract.

The behaviour of an experimental embankment is simulated with the Code_Bright program, considering the atmospheric boundary model, to reproduce the effects of climatic actions in its performance. The results obtain where compared with the measures of TDR sensors installed in the embankment, presenting the importance of taking in to account the climate cycles.

1. INTRODUCTION

In the last decades, the development in the construction of road, and the investigation in the optimization of the resources employed, have led to the reconsideration of the technical specifications applied to the materials, giving the possibility of reutilize the material excavated in the structures of the road.

This reutilization required that this structures been closely monitored with instrumentation, to control the performance of the soil, especially if its behaviour is influenced by the cycles of wetting and drying, in which case the climatic actions are very important.

In the Carmaux (France) road project was necessary to make an excessive excavation compared with the material need for the embankments, for this reason the reutilization of excavated materials in the construction of the structures was considered, one of this embankments was created with the aim of evaluate its behaviour with instrumentation.

2. EMBANKMENT DESCRIPTION.

The site is located at the south of France, in the region of Midi-Pyrénées, the embankment of study is part of the Carmanaux road, and is an experimental embankment which was instrumented to realise a following of the evolution of water content and strains.

The construction was carried out in two stages; the first one was finished in august of 2003, with a height of 10 m, in this phase the equipment for the instrumentation was installed. The second stage begun at the end of 2004 and was finished in April of 2005, Figure 1 presents a scheme of the stages of construction.

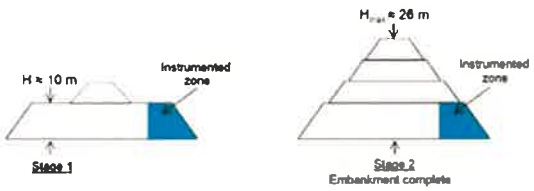

Figure 1 Stages of construction.

As the construction of the road demand a lot of excavations, the material of the zone was used to create the embankment, it was formed by clay with gravels and sandstone, leaven some problems for its reutilization in the road, like:

- Heteroginity of the material
- The proctor test is not representative, because the presence of hard blocks of clay.
- Swelling and degradation of dry soils.

- Deformability of compacted soils in the wet side of the reference proctor test value.

Considering the kind of material used in the embankment can be expected that the variation of moisture in the soil may induce phenomena that result in a fissures or bigger strains in the embankment, such as, cycles of swelling and contraction of the soils, variation in the shear tension in the soil, or changes in the size of the particles due to degradation of the clay blocks. The variation of moisture in the soil was measure by 25 TDR sensors, which approximated location, is presented in Figure 2

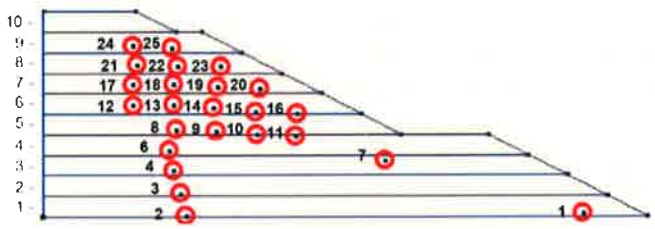

Figure 2 Instrumentation equipment: TDR sensors.

The time of study included the construction of the entire embankment and 18 months more (form august 2003 to October of 2006), the results obtain with the TDR sensors can be compared with the atmospheric data register by the station Albi located at 14 Km south and the station Tanus located 14 Km North of the embankment, in Figure 3 is presented the variation of the volume water content compared with the variation of the atmospheric data, it can be observed that in the first months the water content decrease, the possible reason is that the initial lecture correspond to January of 2004, and that was a winter with abundant rainfall.

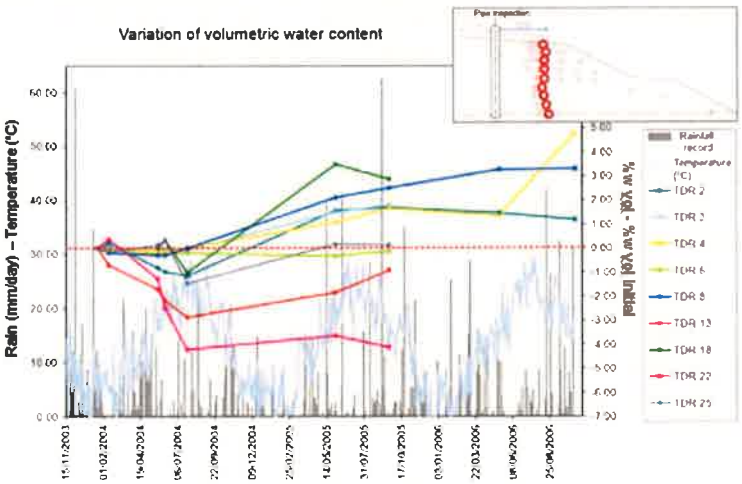

Figure 3 Variation of volumetric water content and atmospheric conditions.

3. MODELLING APROACH.

To achieve a modelling of the embankment construction and analyse the effect of the climatic actions during the construction and the operation of the road (form august 2003 to October of 2006), was used the program of finite elements Code Bright, considering the module of atmospheric boundary conditions.

In order to simplify the modelling, a Thermo-Hydraulic condition was considered, the geometry employed was just the one of the instrumented zone (Figure 4), composed by 1 m layers, the atmospheric data considered are monthly and the mass balance of air equation was not considered.

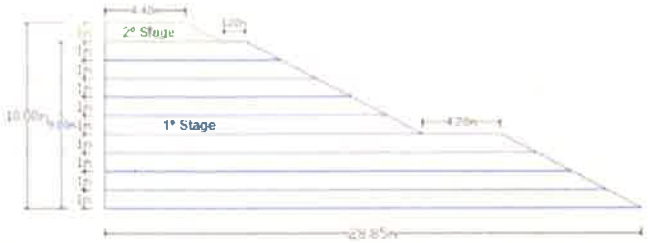

Figure 4 Modelling geometry

The horizontal displacement in the vertical axis were considered none, as the vertical displacement in the base of the embankment, the gas pressure considered was constant and equal to the atmospheric pressure, 0.1 MPa. Even though, the water table is located under the base of the embankment, it was considered a hydraulic condition in the base of the embankment corresponding to a suction of 1M Pa, due to capillary effects. Finally the atmospheric condition is applied to the boundaries that are affected by this effect.

In general the variation of water content in the soil shown with the simulation, present two different zones, the first one located at the upper region presents a decrease in the variation of water content, and the second one, at the lower zone of the embankment presents an increase in the variation of water content, very similar to the general behaviour presented by the TDR sensors. In Figure 5 are presented the comparison between the values of water content obtain with the simulation and the value measured by the TDR sensors at different depth.

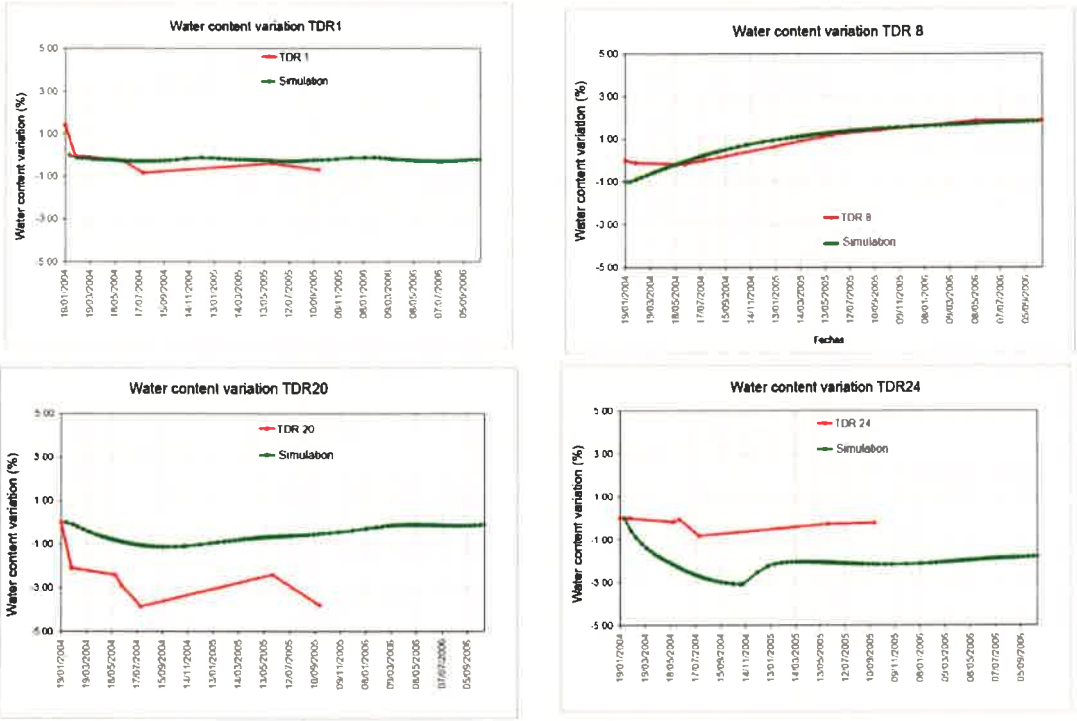

Figure 5 Variation of water content, TDR measures vs. Simulation

4. MODELLING VALIDATION.

Is very important to evaluate if the hypothesis made are acceptable, first of all is important to evaluate if the reduce geometry considered is representative of all the

embankment, for this reason was considered a modelling with the geometry complete, but for the first 200 days, the results of this simulation present that the flux of water at the vertical axis of the reduce geometry are null, validating the hypothesis of the reduce geometry and the waterproof boundary condition imposed at this axis. The heat flux in the axis, present some value in the upper layers of the embankment, which can affect the water content in the upper 2 layers.

The second hypothesis made was the use of a thermo-hydraulic simulation instead a thermo-hydro-mechanic simulation, to verify this, a THM modelling was created, a with a duration of 10 days, the results of this simulation shows the same response of water content as was obtain with the TH simulation. It has little influence because of the high stiffness of the material

The effect of the values of the atmospheric data show that for the considered permeability, the effect of the changes in water at the depth considered to the sensor location (1.5m) is not affected by short events and is sufficient to provide 30 days average values of climate data.

Additionally was evaluated the importance of the atmospheric condition, with this objective a HM modelling without the use of the atmospheric condition was considered. In Figure 6 is presented a comparison between the simulation considering the atmospheric condition (TH simulation) and the one that does not considered it, in terms of water pressure, it can be observed that without considering the atmospheric effects the water pressure tends to an equilibrium value (the value of the suction imposed at the base of the embankment), but with the atmospheric condition the water pressure varies with the climate actions.

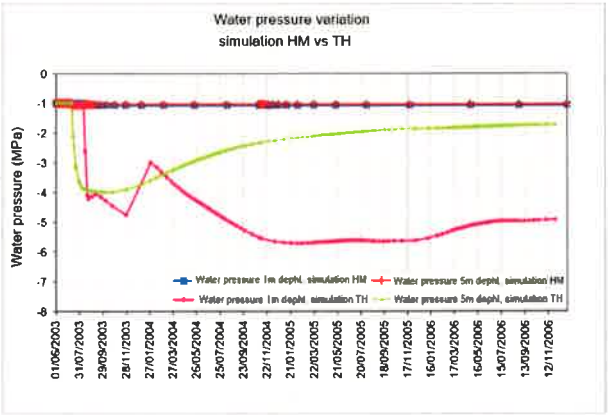

Figure 6 validation atmospheric condition

5. CONCLUSIONS

The simulation of the behaviour of an experimental embankment was achieve, considering some hypothesis to simplify the simulation, was shown that those hypothesis where acceptable and the simulation created was representative of the entire embankment.
Is presented the importance in the analysis the interaction soil-atmosphere especially in no sutured soils where the suction is very important, and susceptible to the moisture changes that can be related to seasonal cycles.

TERMO-MECHANICAL ANALYSIS OF THE STABILITY OF A ROCK-CLIFF UNDER CLIMATIC ACTIONS

D. Ruiz*, J. Vaunat*, S. Samat* and D. Virely†

* Department of Geotechnical Engineering and Geosciences
Technical University of Catalonia (UPC)
Campus Norte UPC, 08034 Barcelona, Spain
E-mail: daniel.ruiz@upc.edu
† Laboratoire Régional des Ponts et Chaussées, France

Key words: Climatic Actions, Heat flux, Rock-cliff, Cavern, Failure, Discontinuities

Abstract. *This paper deals with the numerical analysis of the response of a rock cliff that presents recurrent instabilities as the results of the effect the climatic actions. The Rock cliff is located above an important historic and touristic village, France. It has been recently instrumented in order to detect possible forthcoming failures after the last important damage in 2010. The coupled numerical modelling includes special boundary conditions to involve mass and energy fluxes between the ground and the atmosphere. Finally the response of main discontinuities on the rock mass against the atmospheric conditions is modelled through a special numerical element.*

1 INTRODUCTION

Interactions between the atmosphere and the ground have always been an important issue in civil and geotechnical engineering. Soil-atmosphere interaction is a complex phenomenon that involves balance of heat and different species (liquid water, vapour, air) across the soil surface. Such an interaction has been implemented in CODE_BRIGHT by means of specific boundary conditions (Noilan & Planton, 1989) that impose varying fluxes of evaporation, rainfall, radiation and heat together with changes in atmosphere pressure and temperature.
The analysis aims at understanding the mechanisms responsible of the current deformation of the cliff and its effect on cavity roof stability. As the rock is considered dry, deformations are essentially due to the thermal load caused by solar radiation and changes in air temperature. This case is used to validate, by comparison with field data, the equations for radiation and thermo-mechanical coupling, as well as to provide insights into the stability of fractured rock exposed to the atmosphere (Ruiz et al., 2012; Vaunat et al 2012).

2 MODELLING CLIMATIC ACTIONS

The processes controlling atmosphere conditions include effects of radiation and heat exchange, moist processes (clouds and precipitation), air mass motion and interactions with earth ground components (free surface water, vegetation, outcropping soils and rocks) and therefore the soil-atmosphere interaction is modelled as a boundary fluxes like a precipitation (P), evaporation (E) and solar radiation (Rn) that affect the Thermo-Hydro-Mechanical (THM) coupling process inside the ground.

The Thermo-Hydro-Mechanical processes in soils and rocks fulfilled basic laws of physics, in that case the conservation laws of mass, energy and the stress equilibrium. The general model for the coupled analysis is governed by the conservation laws of three flows (water (1), air (2), energy (3)) and the stress equilibrium (4). The overall coupling processes is presented by Olivella et al. 1994 and Vaunat et al. 2012, where the balance equations with the stress equilibrium ((1) to (4) are formulated and explained.

$$\frac{Dm_w}{Dt} + div(j_w) = f_w \quad (1) \qquad \frac{Dm_a}{Dt} + div(j_a) = f_a \quad (2) \qquad \frac{De}{Dt} + div(j_e) = f_e \quad (3) \qquad div\,\sigma + \rho g = 0 \quad (4)$$

As commented above, the rock is in dry condition; therefore for this particular case it is considered a Thermo-Mechanical coupling which generates deformations due to a conduction heat phenomenon (Fourier law) inside the ground.
The heat flow imposes as boundary condition (atmospheric condition) is presented in the eq (5).

$$j_e = R_n + H_s + H_c \quad (5)$$

where R_n is the net radiation due to the solar energy (short wave, long waves and re-emitted energy), H_s is the sensible heat from heat conduction due to temperature gradient between the rock and the atmosphere and the convective heat H_c generates by the evaporation process across the surface. Because of the low water content (<4%) in the rock, the contribution of the convective flux is negligible.
The sensible heat flux H_s is, calculated through an aerodynamic diffusion relation:

$$H_s = \frac{k^2 v_a \phi}{\ln\left(\frac{z_0}{z_a}\right)^2} \rho_{ga} C_a (T_a - T) \quad (6)$$

where C_a is the specific heat of the air.
Finally the net radiation flux R_n is generated from the direct solar short wave radiation R_g, the long wave atmospheric radiation R_a, the albedo A_l, the emissivity ε and the Stefan-Boltzman constant σ (5.67×10-8 J s-1 m-2 K-4).

$$R_n = (1 - A_l) R_g + \varepsilon R_a - \varepsilon \sigma T^4 \quad (7)$$

$$R_g = \frac{\pi R_G}{2 d_s} \sin\left(\frac{(t - t_m + 0.5 d_s)\pi}{d_s}\right) \quad (8)$$

$$R_a = \sigma T_a^4 \left(0.605 + 0.048\sqrt{1370 \rho_{va}}\right) \quad (9)$$

3 CASE - *LA ROCHE GAGEAC*

3.1 Description and field data

The site concerns a calcareous cliff of Cretaceous age, located in the valley of Dordogne river, France. The cliff culminates at a height of about 100 m above the village of "La Roche Gageac" and is prone to block falls. Several events occurred during the last century (1920, 1954 and 1994). The present study deals with a recent failure that occurs during the winter 2010. It involves a troglodyte cavern, situated at mid-height of the cliff and recognized as a touristic site. Part of the roof fell within the cavern, endangering the historical monument and leaving a rock beam of questioning stability at the crown of the cavern (Figure 1).
Two main families of discontinuities are observed in the massif, possibly controlled by stress release during valley formation and major tectonics directions: 1) a family of decametre-spaced, decimetre wide open fractures oriented parallel to the cliff face and 2) a family of vertical diaclases of millimetre to centimetre width that cut orthogonally the fractures. Opening between essentially horizontal stratification planes and superficial flaking can be observed in the decompression zones above the cavern.
The survey focuses on displacement and temperature monitoring in the cavern and on the cliff upper face. Jointmeters provide relative displacements across the discontinuities delimiting the rock beam within the cavern. Two extensometers provided with thermal sensors and installed in

boreholes drilled horizontally from the cliff face above the cavern (D1 and D2) allow to follow-up displacements and temperature at 2, 4 and 6 m in depth in the rock. Meteorological data are available at a station located at 10 km from the site and near of the cliff. So far they have been measured displacements and temperature in the rock during 2 years with a reversible response in the extensometers and irreversible displacement in two jointmeters located at the extreme of the rock beam (J1 and J2). The Figure 2 shows that displacements of Fissurometers are larger than in distometer by temperature effect.

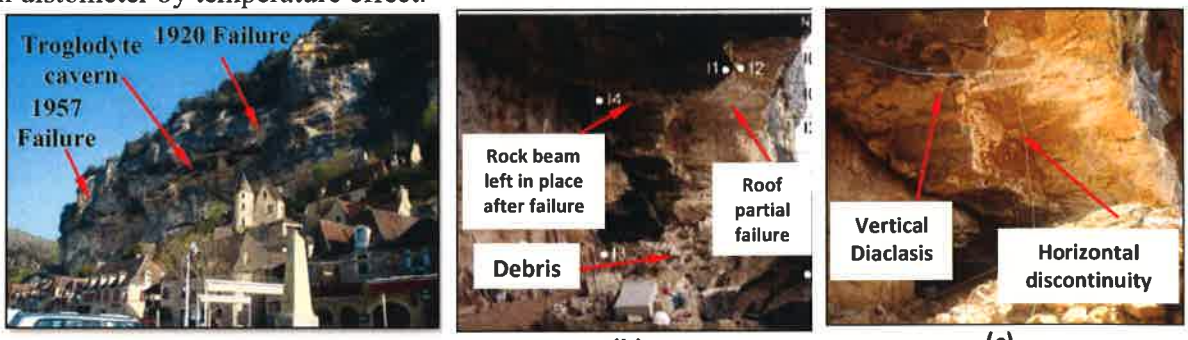

Figure 1: a) General view of the cliff; b) General view of the cavern; c) Beam left in place after the failure

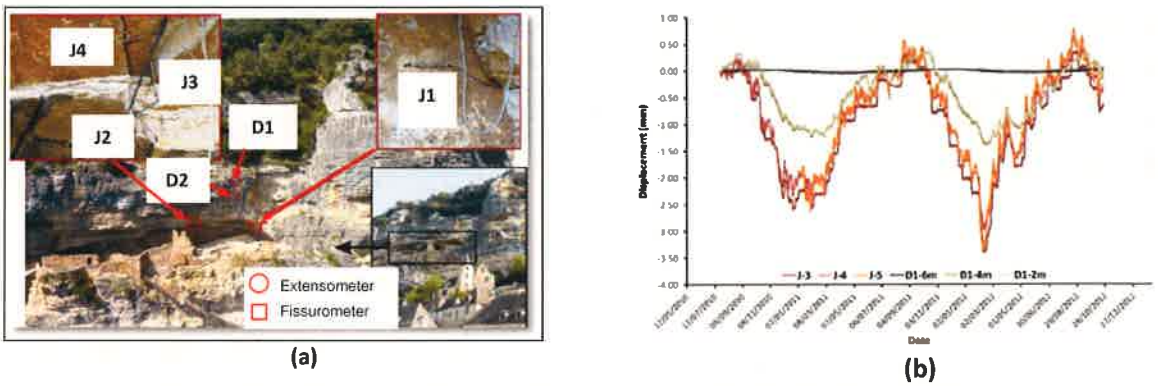

Figure 2: a) Detail of the instrumentation; b) Displacement registers in the extensometers D1 and the Jointmeters.

3.2 Numerical Model

To support the interpretation of instrumentation, a numerical modelling work has been made with the goal to analyze the mechanisms at the basis of the time evolution of displacements and, particularly, of its relationship with temperature. The computation includes only the first year of the atmospheric data (June 2010 to June 2011) where the response of the rock is reversible. The energy fluxes imposed as a boundary condition in the models are presented in the Figure 3.

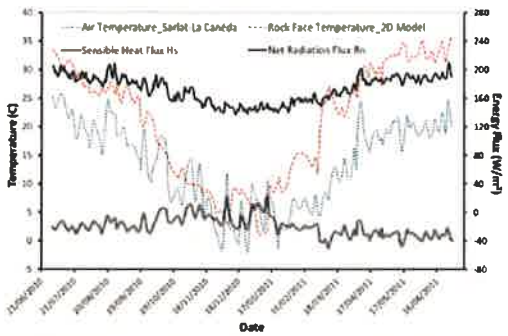

Figure 3: Energy Fluxes generated as boundary conditions

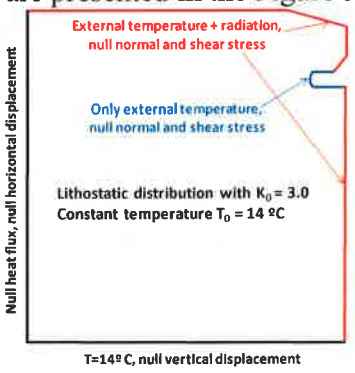

Figure 4: Geometry. Initial boundary - Model 2D

The numerical model considers a vertical section of the cliff passing through the diaclasis previously mentioned (see Fig. 4). Boundaries within the massif have been set at 100 m from cliff face and top, respectively to avoid possible influence on the computation.
From the models (2D and 3D) in which the mechanical model is elastic and including daily atmospheric temperature and solar radiation (both short-wave and long-wave) is simulated the response of the distometers in temperature and displacement (Figure 5). These results shows that the rock mass has an elastic behaviour unlike the discontinuities.

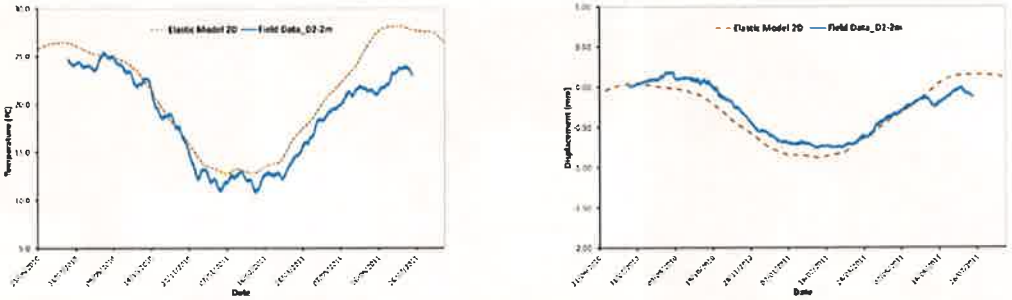

(a) (b)

Figure 5: a) Temperature Distometer 2 – 2m ; b) Displacement Distometer 2 – 2m

Although the behaviour of the discontinuities around the rock beam is irreversible against the threshold of low external temperature, the first year the displacements are reversible and 2D model of roof of the cavern was generated. As a result of the imposition of appropriate boundary condition (The solar radiation is not taken account within the cavern) a good agreement was obtained with the numerical model results (Figure 6). The discontinuities were modelled with the new numerical tool implemented in CODE_BRIGTH which treat the Thermo-Hydro-Mechanical formulation of a contact surfaces.

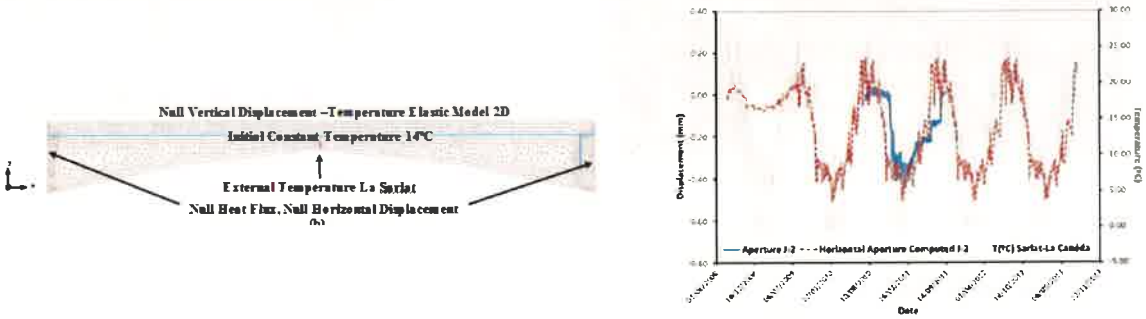

Figure 6: Numerical model of the roof.

4 CONCLUSIONS

This analysis validates the soil-atmosphere model through the comparison with instrumentation and field data and it proof the importance of the solar radiation in the energy balance. Implementation of an elastoplastic model for the joint elements in order to model the irreversible displacement measured is necessary.

REFERENCES

Noilan, J. and Planton, S. 1989. A simple parameterization of land surface processes for meteorological models. Montly Weather Review, vol 117, pp 536-549.

Ruiz, D., Vaunat, J., Samat, S. & Virely, D. 2012. Thermo-mechanical modelling of an aerial cavern under climatic actions. 4th Workshop CODE_BRIGHT, Barcelona.

Ruiz, D. 2013. Thermo-mechanical analysis of the stability of a rock-cliff under climatic actions. Master Thesis, Universitat Politecnica de Catalunya UPC, Barcelona.

Vaunat, J., Samat, S., Alonso, E., Ruiz, D., Martin, E., Saillard, M., Virely, D. & Darrozes, J. 2012. Slope responses under climatic actions. Model and case interpretation. In preparation.

MODELLING HYDRO-MECHANICAL COUPLED PROBLEMS WITH THE MATERIAL POINT METHOD

Alba Yerro[*], Eduardo E. Alonso[*] and Núria M. Pinyol[*†]

[*] Department of Geotechnical Engineering and Geosciences
Technical University of Catalonia (UPC)
Campus Nord UPC, 08034 Barcelona, Spain
e-mail: alba.yerro@upc.edu

[†] Centre Internacional de Mètodes Numèrics en Enginyeria (CIMNE)
Technical University of Catalonia (UPC)
Campus Nord UPC, 08034 Barcelona, Spain

Key words: large deformations, Material Point Method, coupled hydro-mechanical formulation, saturated porous media

Abstract. *Geotechnical problems often involve large deformations and displacements. In order to overcome the difficulties that finite element methods have to reproduce them, other numerical methods such as the Material Point Method (MPM) are being developed. This work presents the features of MPM that make it a useful tool to solve problems involving large deformations and displacements. The mechanical formulation is extended to include hydro-mechanical couplings. Finally some examples of application are solved in the framework of saturated porous media to illustrate the capabilities of the method.*

1 INTRODUCTION

The Material Point Method (MPM)[1] combines the advantages of Eulerian methods such as the finite element methods, with the truly particle methods based on Lagrangian approaches. Two different discretizations of the media are considered: a fixed finite element grid, where the governing equations are solved, and a set of moving material points, where all the information (stress, velocity, pore pressure) is stored. This scheme eliminates mesh distortions, and nonlinear convective terms, troublesome in Eulerian formulations, are not an issue. In addition, this formulation automatically includes a no-slip contact algorithm. All these features make MPM especially useful to solve problems involving large deformations and displacements in geotechnical problems.

In this work the solid skeleton and pore fluid interaction have been taken into account based in the well-known equations described in Zienkiewicz & Shiomi[2] and Verruijt[3], using a formulation based on solid velocity-liquid velocity (v_s-v_f formulation). In addition, two different examples illustrate the dynamic nature of the formulation and the capabilities of the method to model large displacements.

2 MPM COUPLED HYDRO-MECHANICAL FORMULATION

The governing equations of saturated porous media based on v_s-v_f formulation, considering the dynamic problem, are the momentum conservation of the fluid (1) and the momentum conservation of the mixture (2):

$$\rho_f \dot{\mathbf{v}}_\mathbf{f} = \nabla \cdot p\mathbf{I} - \frac{n\gamma_f}{\mathbf{k}}(\mathbf{v}_\mathbf{f} - \mathbf{v}_\mathbf{s}) + \rho_f \mathbf{b} \tag{1}$$

$$(1-n)\rho_s \dot{\mathbf{v}}_\mathbf{s} + n\rho_f \dot{\mathbf{v}}_\mathbf{f} = \nabla \cdot \boldsymbol{\sigma} + \rho_{sat} \mathbf{b} \tag{2}$$

in which $\mathbf{v_s}$ is the solid velocity, $\mathbf{v_f}$ is the real fluid velocity; p is the pore pressure; n is the porosity, $\mathbf{k}$ is the Darcy permeability; ρ_s, ρ_f and ρ_{sat} are the solid, fluid and saturated densities; and $\mathbf{b}$ are the body forces. The Cauchy stress tensor is represented by $\boldsymbol{\sigma}$ and $\mathbf{I}$ is the identity matrix.

The MPM uses two kinds of discretization. Firstly, the initial configuration is divided into a finite number of sub-regions, each one represented by a material point. It is assumed that the whole mass of the specific sub-region (m_p) is concentrated at the corresponding material point. Taking advantage of the definition of Dirac function $\delta(\mathbf{x})$, the mass density field (ρ) can be written as:

$$\rho(\mathbf{x}) = \sum_{p}^{Np} m_p \delta(\mathbf{x} - \mathbf{x}_p) \tag{3}$$

where $\mathbf{x}_p$ is the position of the p^{th} material point and N_p the total number of particles.

Secondly, the equations (1) and (2) discretized using Eq. (3) have to be integrated over the domain using the Galerkin method and discretized on the nodes of a computational mesh considering the standard shape functions.

3 EXAMPLES OF APPLICATION IN SATURATED POROUS MEDIA

3.1 Oedometric Consolidation

Consider the consolidation of a soil defined in Table 1. The sample is a 1m long column, in which a stress of 1 kPa was applied and maintained at the upper boundary. The bottom is impervious.

Material parameter			
Dry unit weight γ (kN/m^3)	23	Porosity n	0.3
Young modulus E (MPa)	10	Water viscosity μ (kg/m·s)	10^{-3}
Intrinsic permeability k (m^2)	10^{-10}	Water bulk modulus K (MPa)	300

Table 1. General characteristics of the tested soil.

The aim of this example is to show the difference between the (static) Terzaghi analytical expression, and the dynamic solution, calculated via the MPM code. Moreover, the effects of damping in the dynamic solution have been analysed.

Two different simulations of the problem were made, the first one is a purely dynamic case and the second one is affected by an extra damping at the bottom, which was imposed with the aim of reaching earlier the static solution.

Figure 1a shows the evolution of the pore pressure along depth at different times for both simulations. Figure 1b provides the evolution of the pore pressure of the material point located at the bottom of the sample. The numerical solution is naturally damped in any case because of the coupling term of the hydro-mechanical formulation, which is explained by water flow through soil pores (at t2 both MPM numerical solutions fit the static solution).

However, the implementation of viscous boundaries (extra damping) is essential to damp the solution as quick as possible if the aim is to capture the quasi-static equilibrium. At t1 (Fig. 1) the MPM solution with extra damping almost reproduces the static solution while the MPM solution with fixed boundary on the bottom still has a strong dynamic behaviour.

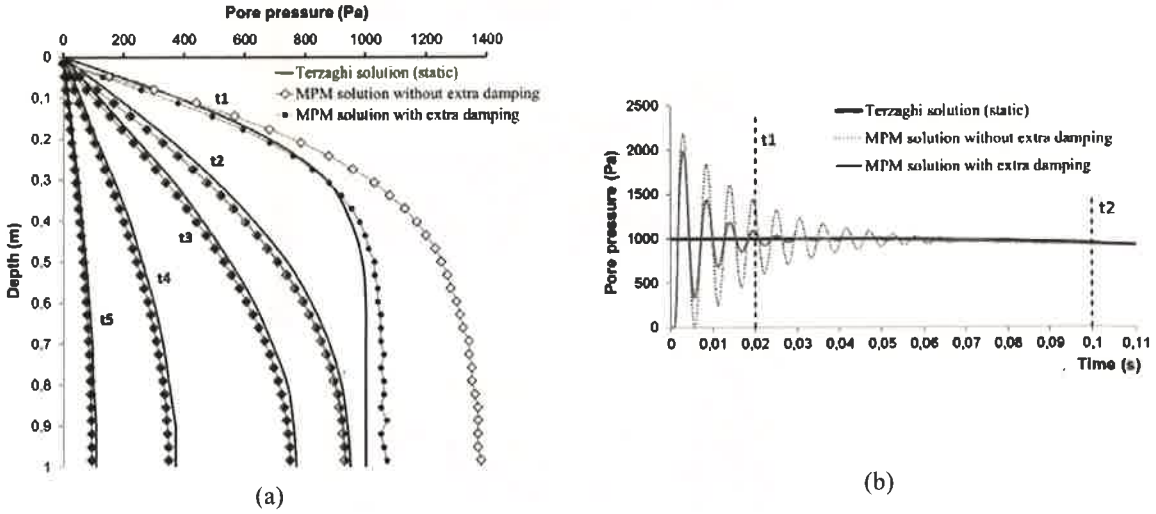

Figure 1. (a) Comparison of analytical and MPM solutions (with and without extra damping on the bottom) for one-dimensional consolidation at different times (t1=0.02s, t2=0.1s, t3=0.2s, t4=0.5s, t5=1s). (b) Evolution of the pore pressure for the deepest material point.

3.2 Slope Instability

This example consists on simulating the instability of a slope, 6 m high and 37° steep due to a rise of the phreatic level. To do that, an increase of the pore pressure (70 kPa) at the lower boundary is imposed. The properties of the material are presented in Table 2, and, in this case, a strain softening Mohr-Coulomb constitutive model is used to simulate its behaviour.

Initially a hydrostatic pressure distribution is assumed and saturated conditions are considered during all the calculation. The excess pore pressure induced by the boundary condition reduces the effective stresses in the slope. This fact, in addition to the strain softening effect, decreases the strength parameters of the material. As a result, the gravitational stresses are sufficient to induce instability. The failure and run-out of the slope is illustrated in Figure 2, where the maximum displacement calculated after the stabilization is 10.9 m.

Material parameter			
Dry unit weight γ (kN/m^3)	20	Porosity n	0.2
Young modulus E (MPa)	20	Cohesion (peak, residual) c_p / c_r (kPa)	1 / 0
Poisson's coefficient ν	0.3	Frictional angle (peak, residual) φ_p / φ_r (°)	35 / 25

Table 2. General characteristics of the soil in slope case

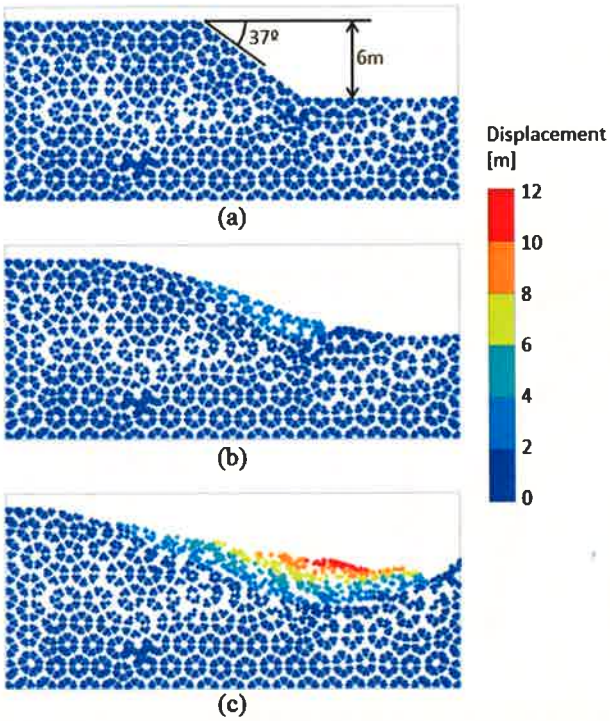

Figure 2. (a) Initial geometry and particle distribution of the slope. (b) Displacements during the instability. (c) Final displacements.

4 CONCLUSIONS

- The hydro-mechanical formulation for the MPM has been outlined
- The MPM is capable of modelling large deformations and displacements

REFERENCES

1. Sulsky, D., Chen, Z. & Schreyer, H. L. A particle method for history-dependent materials. *Computer Methods in Applied Mechanics and Engineering* **118**, 179–196 (1994).

2. Zienkiewicz, O. C. & Shiomi, T. Dynamic behaviour of saturated porous media; the generalized Biot formulation and its numerical solution. *International Journal for Numerical and Analytical Methods in Geomechanics* **8**, 78–96 (1984).

3. Verruijt, A. Theory and applications of Transport in Porous Media. *An Introduction to Soil Dynamics* (2010).

Gas flow in anisotropic claystone. Modelling triaxial experiments

Diego Arnedo, Eduardo Alonso & Sebastià Olivella

Department of Geotechnical Engineering and Geosciences, UPC, Barcelona, Spain

Summary

Selected gas pulse tests on initially saturated claystone samples under isotropic confinement pressure were simulated using a 3D Thermo-Hydro-Mechanical code. The constitutive model considers the hydro-mechanical anisotropy of argillaceous rocks. A cross anisotropic linear elastic law is adopted for the mechanical behaviour. Elements for a proper modelling of gas flow along preferential paths include an embedded fracture permeability model. Rock permeability and its retention curve depend on strains through a fracture aperture. A constitutive internal dimension of the rock structure is required to simulate the aperture of joints. The hydraulic and mechanical behaviour have a common anisotropic structure. Small scale heterogeneity is also introduced in order to enhance the initiation of flow through preferential paths. Simulations are in agreement with recorded upstream and downstream pressures in the tests.

1. Introduction

In this paper, the modelling of two tests performed by Hildebrand et al (2002) [1] is presented. The constitutive model for the rock takes into account its natural cross anisotropy associated with the bedding planes of the rock. This anisotropy is considered both in its mechanical and hydraulic properties. The coupling between the mechanical and hydraulic behaviour of the rock and the possibility of bedding opening due to a decrease of the effective normal stress acting on the bedding planes are substantial improvements over conventional two phase flow models and allow the performance of more accurate analyses of gas flow phenomena in low permeability media such as argillaceous layered rocks.

2. Modelling approach

In The constitutive model for the rock is based on a cross anisotropic model for the mechanical and hydraulic behaviour of the claystone. Two angles describe the orientation of the rock bedding. Bedding has an important effect in the behaviour of this type of rocks since it controls their mechanical behaviour (e.g., highest compressibility in direction perpendicular to the bedding) and their hydraulic properties (e.g., higher fluid conductivity parallel to the bedding planes).

The permeability model used is described in detail in [2]. It simulates the effect of the presence of a planar discontinuity embedded in a given finite element on the value of its permeability. This discontinuity represents, in the cases analyzed in this paper, the bedding planes of the rock, which can be opened due to hydro-mechanical actions (e.g. increase of fluid pressure, effective unloading of the rock). The equivalent element permeability is computed assuming a laminar flow inside the planar fracture.

Figure 1 shows a scheme of the fracture geometry. The orientation of the fracture plane is given by two angles (dip direction angle, α, and dip angle, β). The permeability matrix in the reference cartesian coordinate system is obtained by means of a tensor "rotation", in terms of the intrinsic principal permeability values and the rotation matrices. The principal directions for k_1 and k_2 correspond to the fracture plane, while k_3 follows its normal direction. Changes of fracture aperture are computed through the normal strain to the fracture plane, n being the normal vector

(see figure 1). The mechanical constitutive model is a transversal isotropic elastic model based on the model presented by Wittke [3], which considers 5 material parameters plus 2 anisotropy directions.

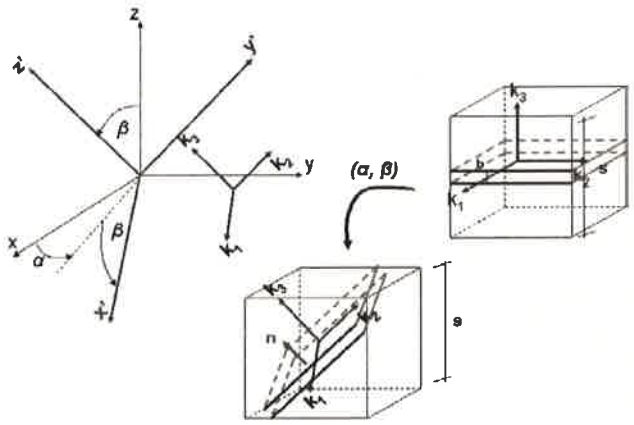

Figure 1. Scheme of the geometry of bedding planes and its relationship with the reference Cartesain coordinate system.

The gas injection on an initially saturated specimen leads to a desaturation of the existing or induced discontinuities. The rock matrix may become also partially saturated. Therefore, the mechanical model should handle the effect of variable suction. The effect of suction is properly accounted for by defining two stress fields: an isotropic one ($s\delta_{ij}$; δ_{ij}: Kronecker delta) and a so called "intergranular stress" which combines total stress and suction. In the model used, a Bishop-like expression defines the average skeleton stress p' in terms of the total mean stress, p, air and water pressures (u_a, u_w) and degree of saturation:

$$p' = p - u_a + S_r(u_a - u_w) = p - u_a + S_r s \qquad (1)$$

The constitutive model used is defined in detail in [4]. Only the elastic anisotropic component was activated in the simulations reported below. In addition, a small scale heterogeneity of the rock has been introduced in an effort to enhance the initiation of the gas flow through preferential paths following the bedding direction. Figure 2 shows a generated spatial distribution of the permeability for k_l (permeability parallel to bedding direction). The distribution is defined in terms of the intrinsic permeability (log scale in the caption; units in m^2). The random field follows a normal distribution (mean value: $9 \cdot 10^{-21} m^2$; variance: $1.3 \cdot 10^{-40} m^4$). This randomness introduces a small variability of permeability.

3. Model validation

To properly simulate the tests a 3D representation of the sample and the upstream and downstream reservoirs (porous metallic stones) is necessary. The sample has been assumed to be cubical in order to facilitate the discretization by means of a structured mesh with cubical elements, which simplifies the hydraulic problem. A sample 30mm high was discretized into 150 quadrilateral linear elemets. The volumes of the two chambers have been adjusted in order to obtain a gas pressure equalisation in the two fluid reservoirs at the end of the simulations which is similar to the value recorded in the experiments.

Two tests were simulated. The first test corresponds to a sample with the bedding planes parallel to the imposed flow (bedding in vertical position), while the in the second test the bedding orientation is horizontal. The first sample was taken from a depth of 1580m, whereas the second sample was taken from a depth of 1515m. The duration of the test is highly dependent on the bedding orientation. The maximum gas permeability recorded is one to two orders of magnitude higher in direction parallel to the bedding than perpendicular to it.

Figure 2 shows the evolution of upstream and downstream pressures for test 1 reported by Hildebrand et al [1] together with the pressures recorded in the test. The overall agreement is good, especially if one considers the evolution of the upstream pressure and the shape of both curves. The increase in the downstream pressure in the simulation of test 1 is delayed about one hour if compared with measurements. The model requires a time lapse for the gas to flow out of the sample into the downstream chamber, while in the actual test the increase in downstream pressure was recorded almost instantaneously.

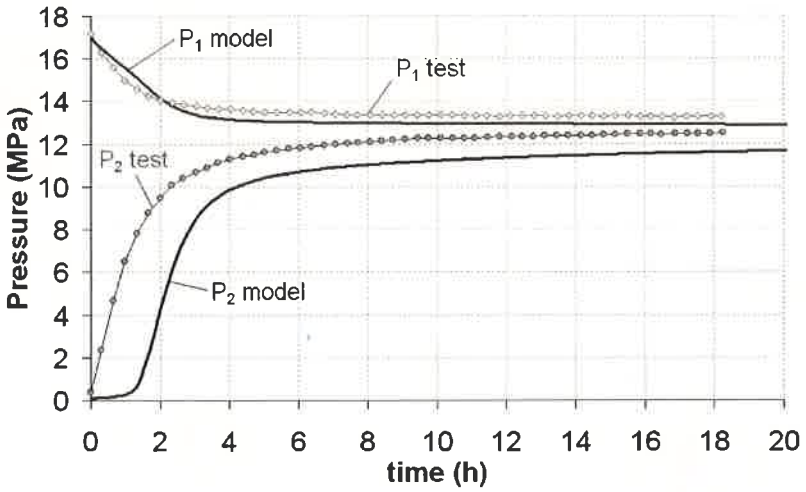

Figure 2. Comparison between simulated and measured pressure evolution at upstream and downstream reservoirs. Test 1.

Figure 3 shows the vectors of gas and water fluxes at a given time of the simulation of test 1. Initially, water flow clearly follows the direction of bedding. Gas and water vectors are at the same scale in figures 3. The effect of bedding opening was clearly visible in the water flux at the beginning of the test. Gas is pushing the water and forcing it to move towards the upper (downstream) reservoir. After the increase in permeability takes place in all the sample elements the vertical flow pattern becomes more homogeneous.

Once the gas pressure exceeds the new capillary air entry value of the material (the retention curve has changed due to deformation) it starts to desaturate the elements during the flow towards the downstream reservoir at the top of the sample.

Figure 4 shows the flow patterns (vectors of gas and water fluxes plotted in a common scale) obtained in the simulation of test 2. The effect of bedding direction is clearly visible and has a strong effect on the fluid flow towards the upper chamber. The orientation of the bedding is horizontal and this fact forces first the water, and afterwards the gas, to flow initially in sub-horizontal direction in each layer of elements.

4. Conclusions

Gas pulse tests on initially saturated claystone samples have been simulated considering the hydro-mechanical anisotropy of the rock. The presence of embedded fractures simulating the rock bedding is included in the permeability model. This is a significant improvement from conventional two phase flow models that allows performing more accurate analyses of gas flow in such type of low permeability layered argillaceous rocks. Two hydro-mechanical simulations of gas tests have been presented. Two bedding orientations, parallel and normal to the imposed flow in the test, have been modelled. Simulations show a good agreement between calculated and recorded pressure evolutions on the two tests.

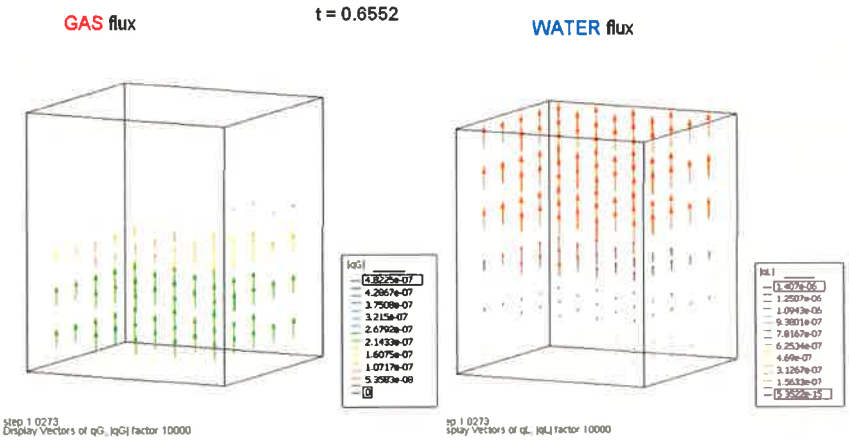

Figure 3. Gas (left) and water (right) advective flow vectors (m/s). Amplification factor 10^4. Test 1. t=0.6552h

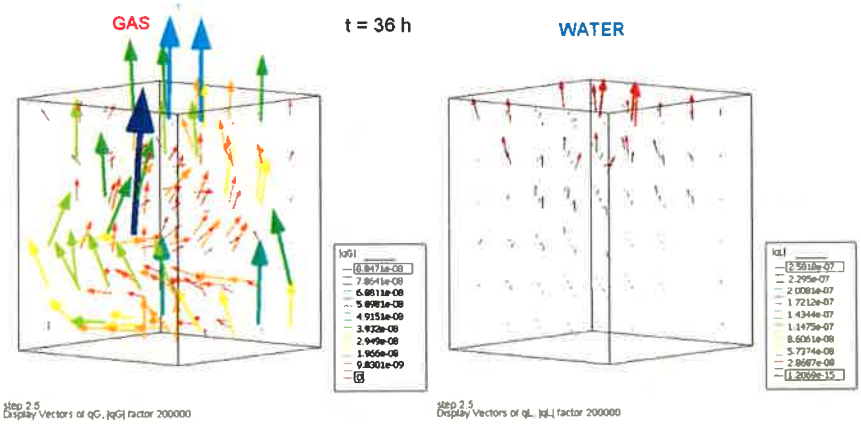

Figure 4. Gas (left) and water (right) advective flow vectors (m/s). Amplification factor $2 \cdot 10^5$. Test 2. t=36h

5. Acknowledgements

This work is funded by the EC through the FP7 research program (FORGE Project).

References

[1] Hildebrand, A., Schlömer, S. & Kroos, B.M., 2002. Gas breakthrough experiments on fine-grained sedimentary rocks. Geofluids: 2, 3-23.
[2] Olivella, S. & Alonso, E.E., 2008. Gas flow through clay barriers. Géotechnique: 58 (3), 157–176.
[3] Wittke, W. 1990. Rock mechanics: theory and applications with case histories. Springer-Verlag.
[4] Gens, A., Vaunat, J., Garitte, B. & Wileveau, Y. , 2007. In situ behaviour of a stiff layered clay subject to thermal loading. Observations and interpretation. Géotechnique: 57 (2), 207-228.

INTERPRETATION OF EVAPORATION TESTS IN CONCRETE COLUMNS BY MEANS OF MULTIPHASE FLOW MODELS

M. Carme Chaparro*, Maarten W. Saaltink*, M. Victoria Villar†

* GHS, Dept. Geotechnical Engineering and Geosciences, Technical University of Catalonia (UPC-BarcelonaTech), Campus Nord UPC, 08034 Barcelona, Spain, e-mail: m.carme.chaparro@upc.edu, maarten.saaltink@upc.edu

† CIEMAT, Centro de Investigaciones Energéticas, Medioambientales y Tecnológicas, Avda. Complutense 40, 28040 Madrid Spain, e-mail: mv.villar@ciemat.es

Key words: evaporation test, multiphase flow, thermo-hydraulic parameters, concrete.

Abstract. *Evaporation tests in concrete columns have been analysed by means of numerical models in order to characterize better the thermo-hydraulic properties and processes in concrete from a Radioactive Waste Disposal Facility in El Cabril (Spain). Heated column (by heating the column with a lamp) and non-heated column (without heating) were used. The conceptual model considers unsaturated liquid flow and transport of vapour and heat. Some models also take into account the salinity in order to study its effect on vapour pressure and evaporation. A retention curve has been obtained from relative humidity and gravimetric water content measured after dismantling the columns. The models have been calibrated by adjusting permeability, thermal conductivity, boundary condition parameters and a tortuosity factor for vapour diffusion to the measured water loss, relative humidity and (in the case of the heated column) temperature. Results show that vapour diffusion is dominant above an evaporation front, and liquid advection is the dominant water transport process underneath this front. The salinity slightly reduces the evaporation.*

1 INTRODUCTION

The durability of concrete in non-saturated conditions is highly bound to evaporation and condensation processes inside concrete. Hence, thermo-hydraulic parameters play an important role. Various methods for measuring these parameters can be found in literature. They include experimental tests for determining retention curves in small samples and in isothermal conditions [i,ii,iii]. For soils methods have been reported that model evaporation tests and calibrate the parameters to experimental data [iv,v]. Although evaporation test in concrete have been reportet[vi] the method of calibration for obtaining thermo-hydraulic parameters has not been applied.

The objective of this work is to obtain thermo-hydraulic parameters of concrete from a Radioactive Waste Disposal Facility in El Cabril (Spain), by modelling evaporation test in concrete columns in non-isothermal conditions.

2 EVAPORATION TESTS

Evaporation tests were performed on concrete columns by CIEMAT [vii] (Fig 1). The tests consisted of letting water evaporate from the top of the column while monitoring water loss by weighing the column, and monitoring temperature and relative humidity by means of 5 sensors placed within the column. One test was performed in laboratory conditions (non-heated column); another one was performed by heating the column with a lamp (heated column), which was situated above the column.

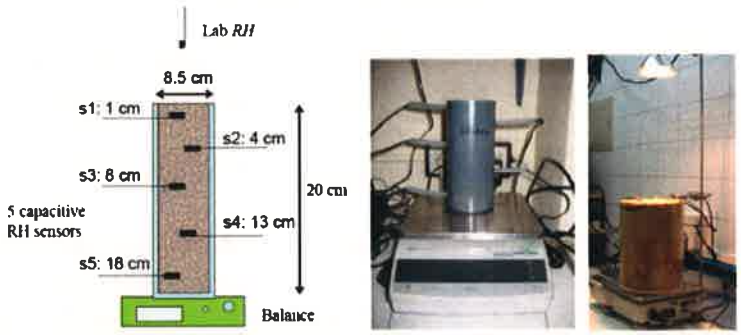

Figure 1: Set up for evaporation tests made by CIEMAT [vii].

3 NUMERICAL MODEL

The conceptual model considers unsaturated liquid flow and transport of vapour and heat. The gas pressure is not considered as a constant. In order to study the effect of the salinity on vapour pressure and evaporation, for each test one model did and another one did not consider salinity. These two assumptions represent extreme cases between which reality is likely to occur, because the model with salinity overestimates salt concentration because it does not account for mineral precipitation.

Calculations were done with CODE_BRIGHT [viii]. The models are one-dimensional. In order to establish boundary conditions, the daily averages of temperature and relative humidity, measured by sensors monitoring laboratory conditions outside the columns were used.

Permeability and porosity were obtained from experimental data from CIEMAT [vii]. The retention curve has been calculated from relative humidity measured by the sensors inside the columns and gravimetric water content measured after dismantling the columns. It was adjusted to the van Genuchten model.

The parameters which are not known or which were more sensitive to the model were calibrated (Table 1). The liquid relative permeability thus obtained drops considerably with saturation, much more than usually found for ordinary granular media, such as soils. However, it resembles the results of Mounlouis-Bonnaire [ix] for gas relative permeability. The tortuosity for diffusive flux was also calibrated. The value obtained from the heated column was higher than that for the non-heated column. This phenomenon has been observed in other experiments and has been called vapour-phase diffusion [x].

Retention curve (van Genuchten law)	$S_e = \left(1+\left(\frac{P_g - P_l}{P_0}\right)^{\frac{1}{1-m}}\right)^{-m}$	$P_0 = 7.7Mpa$ $m = 0.34$	(1)
Liquid relative permeability	$k_{rl} = AS_{el}{}^n$	$A = 0.01$; $n = 7$	(2)
Gas relative permeability	$k_{rg} = AS_{eg}{}^n$	$A = 1$; $n = 3$	(3)
Tortuosity (Fick's law)	$\mathbf{i}^i_{\alpha,dif} = -\left(\tau\phi\rho_\alpha S_\alpha D^i_m \mathbf{I}\right)\nabla\omega^i_\alpha$	$\tau_{non-heated} = 0.08$ $\tau_{heated} = 0.3$	(4)
Thermal Conductivity (Fourier's law)	$\mathbf{i}_c = -\lambda\nabla T$ $\lambda = \lambda_{sat}{}^{S_l}\lambda_{dry}{}^{(1-S_l)}$ $\lambda_{sat} = \lambda_{solid}^{(1-\phi)}\lambda_{liq}^{\phi}$ $\lambda_{dry} = \lambda_{solid}^{(1-\phi)}\lambda_{gas}^{\phi}$	$\lambda_{solid} = 1.3\ WmK^{-1}$ $\lambda_{gas} = 0.024\ WmK^{-1}$ $\lambda_{liq} = 0.6\ WmK^{-1}$	(5)
Exchange vapour coefficient (vapour flux equation)	$j^w_g = \left(\omega^w_g\right)^0 \gamma_g \left(P^0_g - P_g\right) +$ $+\beta_g\left[\left(\rho_g\omega^w_g\right)^0 - \left(\rho_g\omega^w_g\right)\right]$	$\beta_g = 10^{-3} ms^{-1}$ $\beta_g = 3.7{\cdot}10^{-2} ms^{-1}$	(6)

Table 1: Parameters calibrated in the model

4 RESULTS AND DISCUSSION

Comparing both models for the non-heated column, the results of relative humidity, loss of weight and fluxes are similar for both models due to the fact that evaporation and, therefore, salinity is low. In the heated column the salinity effect is more important because of the higher evaporation. Results of loss of weight show a reduction of about 5% due to salinity. At the upper part of the heated column relative humidity is lower for the model with salinity, because salinity is higher (Psychrometric law). At the lower part of the column, relative humidity is higher, because saturation is higher and, consequently salt concentration is lower. Though both models represent two extreme cases, the model with salinity resembles better the experimental data.

In both columns, the flux results show that vapour diffusion is dominant above an evaporation front, and liquid advection is the dominant water transport process below it. Gas advection appears above the evaporation front but is of minor importance. In the heated column, high salinity produces less evaporation for the model with salinity and therefore high saturation. So vapour diffusion is lower and liquid advection is higher.

5 CONCLUSIONS

Evaporation tests were performed in concrete columns. They have a long duration but a simple design. The thermo-hydraulic multiphase flow models of these evaporation tests help to understand processes in concrete.

The calibration of models made it possible to obtain thermo-hydraulic parameters. The retention curve obtained shows that this concrete is a very retentive material reflected by the

high entry pressure obtained (P_0 Table 1). The liquid relative permeability drops considerably with saturation in comparison to a granular media. Difference in tortuosity of both models indicated enhanced vapour diffusion.

Salinity slightly reduces evaporation. This reduction acquires importance when evaporation from the column is higher. In both columns, vapour diffusion is dominant water transport above the evaporation front and liquid advection is dominant below it.

Acknowledgement. This work was funded by ENRESA (Spanish Nuclear Waste Management Company) and a Research Grant from the Technical University of Catalonia (UPC).

6 REFERENCES

[i] Leech, C., D. Lockington, R. D. Hooton (2006), Estimation of water retention curve from mercury intrusion porosimetry and van Genuchten model, ACI Structural Journal, 103(2), 291-295.

[ii] Baroghel-Bouny, V. (2007), Water vapour sorption experiments on hardened cementious materials Part I: Essential tool for analysis of hygral behaviour and its relation to pore structure, Cement and Concrete Research, 37, 414-437.

[iii] Carlier, J.Ph., N. Burlion (2011) Experimental and numerical assessment of the hydrodynamical properties of cementitious materials, Transp Porous Med, 86, 87-102.

[iv] Pintado, X., A. Ledesma, A. Lloret (2002), Backanalysis of thermohydraulic bentonite properties from laboratory test, Engineering Geology, 64, 91-115.

[v] Gran M., J. Carrera, S. Olivella, M.W. Saaltink (2011), Modeling evaporation processes in a saline soil from saturation to oven dry conditions. Hydrology and Earth System Sciences, 15, 2077-2089.

[vi] Selih, J., A. Sousa, T.W. Bremner (1996), Moisture Transport in Initially Fully Saturated Concrete During Drying. Transport in Porous Media, 24, 81-106.

[vii] Villar, M.V., P.L. Martín, J.M. Barcala (2009), Caracterización del material de cobertera y el hormigón del C.A. El Cabril, Informe Técnico CIEMAT/DMA/2G205/03/09, CIEMAT, Madrid, 55pp.

[viii] Olivella, S., A. Gens, J. Carrera, E.E. Alonso (1996), Numerical formulation for a simulator (CODE_BRIGHT) for the coupled analysis of saline media, Eng. Comput.,13(7), 87-112.

[ix] Monlouis-Bonnaire,J., J. Verdier, B. Perrin (2004), Prediction of the relative permeability to gas flow of cement-based materials Cement and Concrete Research, 34, 737-744.

[x] Clifford, K., S.W. Webb (1996), A Review of Porous Media Enhanced Vapor-Phase Diffusion Mechanisms, Models, and Data-Does Enhanced Vapor-Phase Diffusion Exist? Geohydrology Department, Sandia National Laboratories.

MODELLING CRYSTAL GROWTH

A. RAMON[*†], **E. ALONSO**[*]

[*] Department of Geotechnical Engineering and Geosciences
Technical University of Catalonia (UPC)
Campus Nord UPC, 08034 Barcelona, Spain
e-mail: anna.ramon@upc.edu, eduardo.alonso@upc.edu

[†] International Center for Numerical Methods in Engineering (CIMNE)
Edificio C1, Campus Nord UPC
Gran Capitán s/n, 08034 Barcelona, Spain

Key words: Gypsum, crystal growth, swelling phenomena, HMQ coupled analysis

Abstract. *The sustained heave of Pont de Candí Bridge is a consequence of the development of swelling strains in the sulphated claystone located below the tips of the foundation piles of the central pillars of the bridge. The development of swelling phenomena in sulphated claystone is explained by the precipitation of gypsum crystals in fractures. A model has been formulated to describe the kinetics of precipitation and dissolution of sulphated minerals, the development of strains induced by crystallization and the solute transport. The heave of Pont de Candí Bridge has been modelled and calculations have been compared with the field measurements.*

1 INTRODUCTION

The central pillars of Pont de Candí railway bridge experienced a significant heave at rates ranging from 5 to 10 mm/month immediately after its construction[i]. Long continuous extensometers installed near the central pillars of the bridge identified the development of swelling strains below the tip of piles, in a hard Eocene anhydritic claystone formation (Figure 1). Swelling deformations accumulated in an active layer, 9-15 meters thick, located along the axis of the bridge. The deep expansion resulted in significant ground surface heave (9-13 mm in 5 months). An embankment 33 m high was built covering partially the valley to remediate the heave of the structure. The heave rate decreased after the construction of the embankment but it was not eliminated (Figure 1).

2 SWELLING MECHANISM

Swelling phenomena in sulphated clayey rocks are explained by the precipitation of gypsum crystals in open discontinuities[i]. The presence of anhydrite plays a central role in the phenomenon. Since the solubility of anhydrite ($CaSO_4$) is higher than the solubility of gypsum ($CaSO_4 \cdot H_2O$) at the temperatures prevailing in the field, water in contact with the anhydritic clayey rock will tend to dissolve anhydrite and therefore the excess of calcium sulphate dissolved (with respect to the solubility of gypsum) will tend to precipitate as gypsum crystals. Joints provide a favourable environment for crystal growth. The process of precipitation of gypsum in discontinuities is thought to act as a local jacking effect pushing apart the rock mass, opening discontinuities and inducing swelling strains.

Hydraulic cross-hole tests performed in the area of Pont de Candí viaduct revealed the existence of horizontal hydraulically connected fractures in the active layer which provided

the necessary open space for gypsum crystals to grow and also confirmed the presence of circulating water. Above and below the active layer a sharp decrease of the permeability was found.

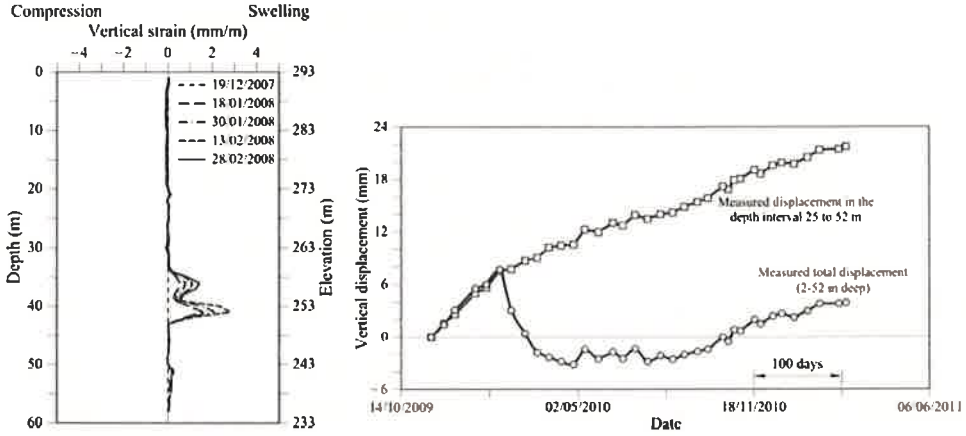

Figure 1. (a)Vertical strains measured by a sliding micrometer between Pillars P4 and P5 before the construction of the embankment; (b) Evolution of the integral of vertical strains measured between pillars P6 and P7 by a sliding micrometer before and after the construction of the embankment

3 MODEL FORMULATION

The direction and intensity of deformations induced by precipitation of crystals will be controlled by the geometry of fracture families (Figure 2a and Figure 2b).

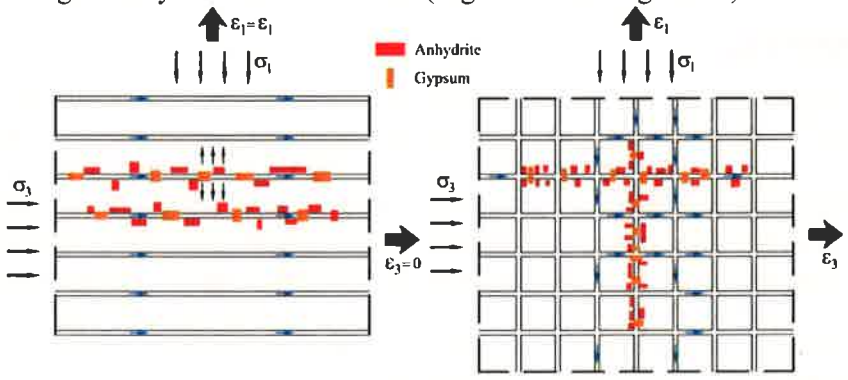

Figure 2. A "representative element" of sulphated rock for (a): swelling in vertical direction, (b): swelling in two directions

The phenomenon has been formulated within a general framework of hydromechanical analysis for saturated and unsaturated porous media[III]. The material involved in the swelling mechanism is not a standard material. The solid phase of the porous rock made up of an insoluble clay matrix and two soluble minerals, gypsum and anhydrite, which may dissolve and precipitate. Solid mass balance leads to:

$$\frac{D_s\phi}{Dt} = (1-\phi)\nabla\cdot\left(\frac{d\boldsymbol{u}}{dt}\right) - \frac{1}{\rho_{gyp}}\frac{dm_{gyp}}{dt} - \frac{1}{\rho_{anh}}\frac{dm_{anh}}{dt} \qquad (1)$$

Eq. 4 indicates that the variation in porosity in time has two components, the volumetric strain rate induced by solid displacements and the volumetric strain rate induced by the precipitation or dissolution of crystals.

The processes of dissolution and precipitation of minerals are described by means of two

mass rate equations depending on the concentration of sulphates dissolved in water, temperature and, also, pressure[iv]. In the case of gypsum kinetics:

$$\frac{dm_{gyp}}{dt} = \sigma_c \kappa \xi_{gyp} \phi_{gyp} \left(\left| \left(\frac{\omega_l^m}{\omega_{l_{sat\_gyp}}^m (T,p)} \right)^\theta - 1 \right| \right)^\eta , \qquad \xi_{gyp} = \frac{\omega_l^m - \omega_{l_{sat\_gyp}}^m}{\left| \omega_l^m - \omega_{l_{sat\_gyp}}^m \right|} \tag{2}$$

The mass conservation of solute is formulated for calcium sulphate, the sole solute in this case:

$$\begin{aligned} &\rho_l \omega_l^m \nabla \cdot \left(\frac{du}{dt} \right) + \phi \frac{D_s \left(\rho_l \omega_l^m \right)}{Dt} + \nabla \cdot \left(\rho_l \omega_l^m q_l - \boldsymbol{D} \nabla \cdot \omega_l^m \right) = \\ &= -\frac{dm_{gyp}}{dt} \left(1 - \frac{\rho_l \omega_l^m}{\rho_{gyp}} \right) - \frac{dm_{anh}}{dt} \left(1 - \frac{\rho_l \omega_l^m}{\rho_{anh}} \right) \end{aligned} \tag{7}$$

The precipitation and dissolution of sulphated minerals are treated as a source or sink of calcium sulphate solute.

The strains induced by precipitation of gypsum are calculated from the amount of precipitated volume of gypsum and the prevailing stress acting on crystals, and are considered as imposed deformations.

$$\frac{d\varepsilon_i}{dt} = \frac{\gamma_i}{\rho_{gyp}} \frac{dm_{gyp}}{dt} \qquad , \quad i = 1,\ 2,\ 3 \ \ ;\ 1 = Vertical\ (z)\ \ ;\ 2,\ 3 = Horizontal\ (h) \tag{8}$$

The parameter γ_i is a coefficient that takes into account the effect of the stress applied on crystals on the strains induced by precipitation. It will be assumed to be controlled by stress.

This formulation was included into CODE BRIGHT[ii].

4 SIMULATION OF EXPANDING MECHANISM BELOW PONT DE CANDÍ FOUNDATIONS

A column of the foundation material at the central pillar of the bridge (P5) has been modelled under plane strain conditions[iii]. The active layer was included at the position estimated by the sliding micrometers. The horizontal flow conditions in the active layer were reproduced. The fractured and highly permeable sulphated claystone was modelled as a porous material. The compound kinetic coefficient, $\sigma_c \cdot \kappa$, was back calculated by matching the swelling records with the calculated heave. The initial open porosity (0.09) was higher than the rock matrix porosity to account for fissures. An intrinsic permeability of $2 \cdot 10^{13}$ m^2, found in the cross-hole hydraulic tests, was adopted for the active layer. An isotropic linear elastic behaviour was considered for the material of the column.

The calculated vertical displacements reproduced the field heave records in the four years period modelled. The construction of the embankment was simulated by applying a loading at the upper boundary of the column. The model reacts to embankment construction and the calculated vertical displacement reproduces the field measurements recorded after the "construction" of the embankment (t=924 days in Figure 3).

A sensitivity analysis performed indicates that the initial mineral content has an important effect on the development of heave because it controls the rates of dissolution and precipitation (Eq. 2). Anhydrite content has a higher effect than gypsum content. The value of equilibrium concentration at saturation with respect to gypsum and anhydrite, which depends

on temperature, has also a significant effect on vertical strains. Stress effects are substantial in the model developed. In contrast, the initial porosity, the permeability and the induced gradient have minor effect on the calculated heave.

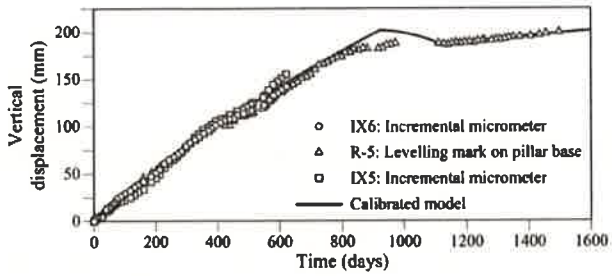

Figure 3. Measured and calculated surface heave.

5 CONCLUSIONS

Field investigations carried out in the valley where Pont de Candí bridge was built demonstrated that the existence of an expanding layer located below the tips of the piles originated the heave of the structure and the surrounding ground surface.

The swelling process is related with gypsum crystallization in fissures. The crystallization of gypsum in discontinuities produces a jacking effect pushing upwards the soil and rock layers above the active zone, as well as the bridge pillars. The hydraulic connection in the active expanding layer explains the presence of water and the existence of fractures, necessary for gypsum crystal growth.

A model was developed for simulating the expansion in sulphated rocks due to gypsum crystal growth. The presence of soluble sulphated minerals and the occurrence of precipitation and dissolution of crystals have been considered in the formulations. The sensitivity analysis performed indicated that the initial anhydrite and gypsum content, solubility of gypsum and anhydrite and, especially, the confining stress have a relevant effect on the swelling strains calculated in the model developed. A simulation of the conditions in the foundation material of Pont de Candí has been performed. Measured heave is reproduced by the model. The tool developed is believed to constitute a step forward in the analysis and prediction of swelling phenomena in sulphate bearing clay rocks.

6 AKNOWLEDGEMENTS

The support and funding provided by the Spanish National Agency for Railway Infrastructure (ADIF) is highly appreciated.

REFERENCES

[i]. Alonso, E. E. & Ramon, A. (2012). Heave of a railway bridge induced by gypsum crystal growth: field observations. Géotechnique, ahead of print http://dx.doi.org/10.1680/geot.12.P.034.

[ii]. DETCG (2010). CODE_BRIGHT User's Guide. Available on-line: https://www.etcg.upc.edu/recerca/code_bright.

[iii]. Ramon, A & Alonso, E. (2012). Heave of a railway bridge modelling of gypsum crystal growth. Géotechnique ahead of print. http://dx.doi.org/10.1680/geot.12.P.035

[iv]. Scherer, G. (1999). Crystallization in pores. Cem. Concr. Res. 29, 1347-1358.

MODELLING 3D MECHANICAL INTERFACES WITH CONTINUUM ELEMENTS

Damians I.P.*, Olivella S.*, Lloret A.*, Josa A.*, and Bathurst R.J.†

* Department of Geotechnical Engineering and Geosciences
Universitat Politècnica de Catalunya – BarcelonaTech (UPC)
Campus Nord UPC, 08034 Barcelona, Spain
E-mail: ivan.puig@upc.edu

† GeoEngineering Centre at Queen's-RMC, Civil Engineering Department
Royal Military College of Canada (RMC)
K7K 7B4 Kingston, Ontario, Canada

Key words: Mechanical interfaces, Reinforced soil–retaining walls, Pullout

Abstract. *This document presents preliminary results of FEM-numerical analysis of soil-reinforcement pullout tests. The numerical model has been developed with CODE_BRIGHT and assuming the interfaces as continuum materials. The results of the preliminary parametric analyses described herein provide useful information on the shear behavior modeling of soil-reinforcement strip interfaces under working stress conditions.*

1 INTRODUCTION

Accurate design of reinforced soil-retaining walls requires knowledge of the actual interface shear behavior of the reinforcement elements. Typically, these types of structure operate under working stress conditions (i.e. far away from failure), so they do not generate enough strain to fully develop soil-reinforcement interface strength. Nevertheless, interfaces must have adequate stiffness and shear strength. Therefore, pullout tests are particularly useful to examine interface behavior and to quantify interface stiffness and strength. These parameters allow reinforcement design optimization to be carried out and/or to determine an adequate number of reinforcement elements to ensure safety.

Several FE models have been developed to analyze these types of structures and interface behavior [1]. For steel reinforcement and also rough polymeric strips, interfaces are assumed to be rigid (i.e. perfectly bonded to the surrounding soil). This approach is consistent with back-calculated pullout shear resistance reported in the literature [2].

2 NUMERICAL MODEL OF PULLOUT

2.1 Model features: materials, properties and boundary conditions

Figure 1 shows the 3D numerical model mesh geometry developed to analyze the pullout behavior of a steel strip placed in a box with appropriate box dimensions to minimize boundary effects. The reinforcement has typical strip dimensions. The model has 1652 nodes corresponding to 1350 quadrilateral elements. As can be observed, the reinforcement-backfill interface has been modeled assuming a certain thickness of continuum elements.

The calculation process takes two stages: The first one corresponds to an initial equilibrium state (steps from 0 to 10, taking one day), and the application of the pullout load (steps from 10 to 11, taking another day). The pullout has been modeled by prescribing a constant velocity-displacement to the front of the reinforcement strip at the beginning of the second stage (i.e. step 10), which generates about 20 cm of pullout displacement at the end of the stage (i.e. at the end of the step 11). No external surcharge pressures have been considered in the analyses.

With respect to the remaining boundary conditions, displacements in the orthogonal directions are not allowed, with the exception of the top-horizontal surface and the interface areas at front and back surfaces (no prescribed conditions), and the reinforcement (which has the prescribed pullout displacement at the front, and free-end displacement at the back).

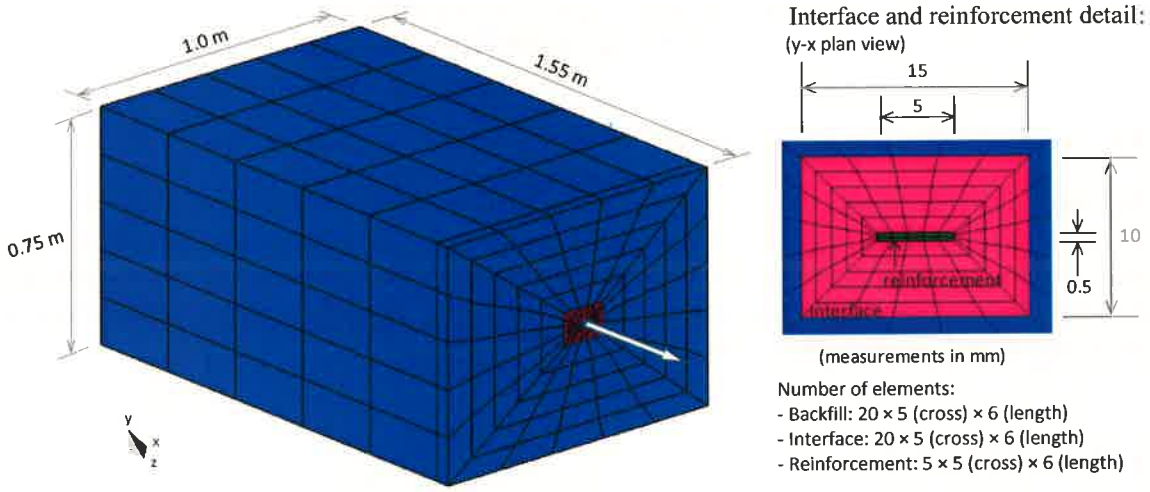

Figure 1: FE - 3D model mesh and geometry dimensions

Table 1 presents the constitutive model material parameters. As can be observed, the reinforcement material has been modeled as a linear elastic material, which is a good assumption for steel reinforcements (e.g. steel strips or ladders). Soil materials (i.e. the backfill soil and the soil-reinforcement interface) have been modeled with a linear elastic stiffness (Young's modulus and Poisson's ratio parameters) plus a visco-plastic law at strength-failure, which is controlled by the cohesion, friction angle and dilatancy angle. A suitably low viscosity value has been selected so that viscous effects do not influence numerical outcomes.

	Materials					
Parameters	Reinforcement	Backfill		Interface		Units
Solid phase density	75	27		27		kN/m^3
Porosity, n	0.001	0.3		0.3		-
Young's modulus, E	210 000	20		20		MPa
Poisson's ratio, ν	0.3	0.3	0.05	0.3	0.49	-
Cohesion, c	-	0.001		0.001		MPa
Friction angle, ϕ	-	45	45 (rigid)	31 (= 0.6ϕ)	17 (= 0.3ϕ)	degrees
Dilatancy angle, ψ	-	15	15	1	0	degrees

Table 1: Constitutive model material parameters

2.2 Results

Figures 2 and 3 present the results of the base case, which corresponds to a rigid interface case and v = 0.3 (i.e. same properties as the surrounding material). As can be observed in Figure 2, pullout displacements generate significant vertical displacements due to dilatancy effects. This effect becomes more significant at both edges of the reinforcement due to the boundary conditions of prescribed displacements, but it is not caused by the axial strains of the reinforcement (which can be assumed as inextensible). Results of the stresses and strains of the backfill and interface at different reinforcement length locations can be observed in Figure 3. Vertical stresses are also the result of dilatancy behavior, increasing in value around the vertical sides of the reinforcement strip with respect to soil overburden pressure.

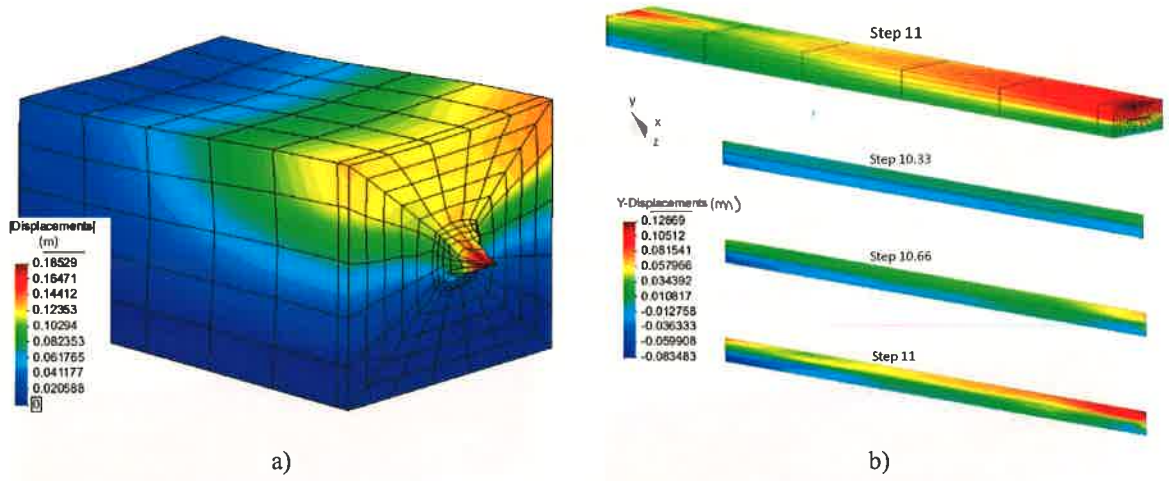

Figure 2: Rigid interface case with v = 0.3: Total displacements and deformed mesh (a) and vertical displacements results (b) with their evolution in time on interface cross-length-section

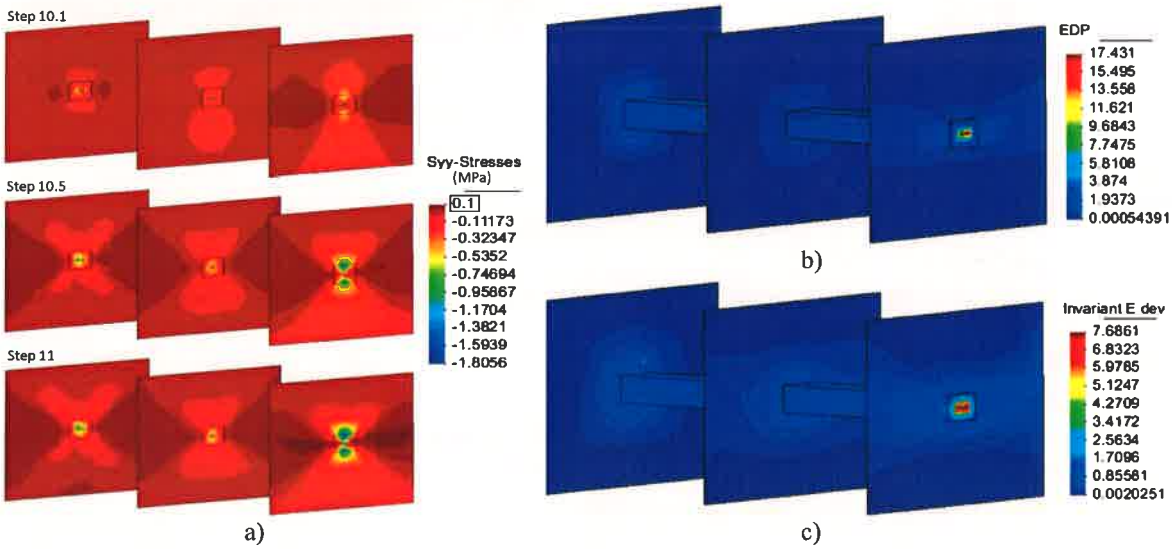

Figure 3: Rigid interface case with v = 0.3: (a) vertical stress, (b) plastic shear strains and (c) total shear strains, over three cross-lateral-sections of backfill and interface materials

Figure 4 presents the results of the pullout axial stress at the edge of the reinforcement with respect to axial displacement, for the three cases of interface Poisson's ratio ($0.05 - 0.3 - 0.49$), for each case of interface strength reduction ($rigid - 0.6\phi - 0.3\phi$). Poisson's ratio appears to have little influence on interface performance for the assumed conditions. Figure 5 shows the total shear strains according to the interface strength and $v = 0.3$. As can be observed, the less the interface strength (e.g. 0.3ϕ case), the more clearly defined the shear zones (i.e. failure surfaces) that are generated due to the pullout.

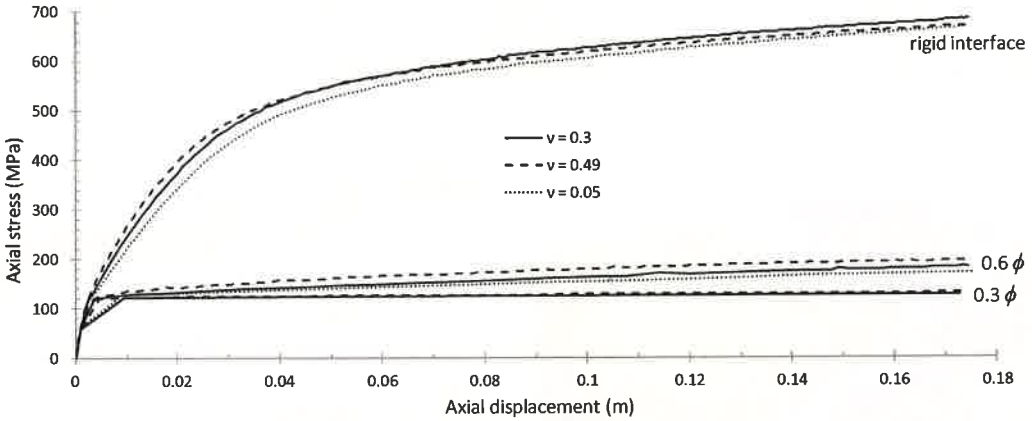

Figure 4: Axial stress-displacement responses

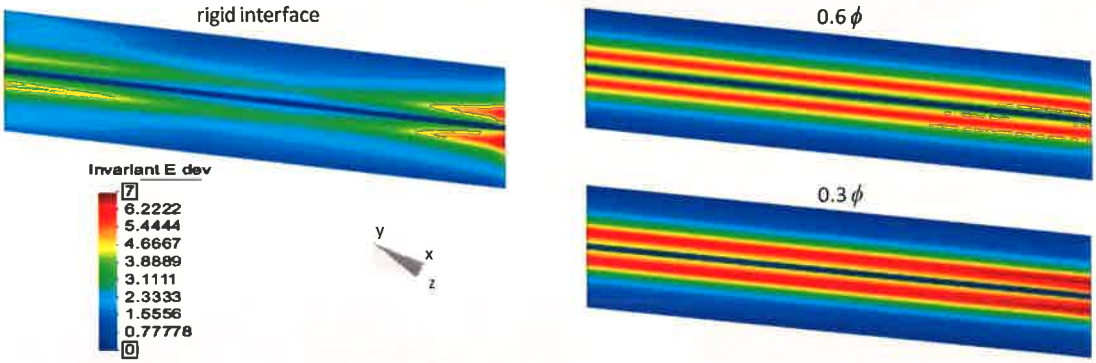

Figure 5: Total shear strains at interface due to pullout. Failure surface generation

3 CONCLUSIONS

- The numerical 3D model for steel reinforcement pullout appears promising for future analyses.
- Soil behavior trends observed are in agreement with experimental data.

REFERENCES

[1] Damians, I.P., Bathurst, R.J., Josa, A., Lloret, A. and Albuquerque, P.J.R. 2013. Vertical facing loads in steel reinforced soil walls. ASCE Journal of Geotechnical and Geoenvironmental Engineering (in press).

[2] Miyata, Y. and Bathurst, R.J. 2012. Analysis and calibration of default steel strip pullout models used in Japan. Soils and Foundations, Vol.52, No.3, pp. 481-497.

MODELLING COMPACTED SOILS INCLUDING MICROSTRUCTURAL FEATURES

Núria M. Pinyol[*†], **Eduardo E. Alonso**[†] **and Antonio Gens**[†]

[*] International Center of Numerical Methods in Engineering (CIMNE)
Technical University of Catalonia (UPC)
Building C1, Campus Nord UPC
Gran Capitan s/n, 08034 Barcelona, Spain
e-mail: nuria.pinyol@upc.edu, web page: http://www.cimne.com

[†] Department of Geotechnical Engineering and Geosciences
Technical University of Catalonia (UPC)
Building D2, Campus Nord UPC
Gran Capitan s/n, 08034 Barcelona, Spain
e-mail: eduardo.alonso@upc.edu, antonio.gens@upc.edu web page: http://www.etcg.upc.edu/

Key words: compacted soils, double structure, constitutive stress, effective degree of saturation

Abstract. *The behavior of a compacted soil depends on the compaction conditions in terms of the applied stress and water content which lead the soil to a particular dry density and suction. In addition, soil properties also depend on the microstructure generated during compaction. To take these features into account, this paper presents a model which includes the microstructure as a state variable. Details of the performance of this model, which has a relatively simple elastoplastic formulation, are presented. The simulation of isotropic stress paths illustrates the capabilities of the model and the effect of the microstructural state variable.*

1 INTRODUCTION

It is commonly accepted that the observed differences in the mechanical and hydraulic properties of a compacted soil are essentially controlled by the compaction conditions in terms of dry density and water content. In modeling, both conditions are generally introduced as initial stresses (density is usually linked with preconsolidation stress and water content with suction). However, in addition to the effect of compaction density and suction, soil properties also depend on the microstructure generated during compaction. Microstructural properties have been introduced in constitutive modeling more recently by several authors [i,ii,iii]. In the model presented in this paper, the soil microstructure is incorporated following the ideas presented by Alonso et al. (2010)[ii].

The soil microstrucure is quantified by a single parameter, ξ_m, the ratio of the microstructural void ratio (intra-aggregate space) and the total void ratio. Microstructural void ratio can be determined, following the proposal of Delage and Lefebvre (1984) [iv], if intrusion-extrusion curves of MIP are available.

The parameter ξ_m is used in the definition of an effective degree of saturation as follows:

$$\bar{S}_r = \frac{S_r - \xi_m}{1-\xi_m} + \frac{1}{n}\ln\left[1+\exp\left(-n\frac{S_r-\xi_m}{1-\xi_m}\right)\right] \qquad (2b)$$

where n is a smoothing parameter.

The basic idea behind this equation is that only the water partially filling the macropores will have a significant mechanical effect on soil ([11])

2 MODEL HYPOTHESIS AND MODEL FORMULATION

The formulation of the constitutive model can be interpreted as a modification of Barcelona Basic Model, BBM[v] formulated in terms of two stress variables:

- Effective stress: $\bar{\sigma} = \sigma - p_g + \bar{S}_r s$ (2)
- Effective suction: $s_{ef} = S_r^c s$ (3)

where p_g is the air pressure, $\bar{S}_r$ the effective degree of saturation defined in Eq. (1) or (2) and s, the matric suction.

Elastic and plastic volumetric changes in void ratio (e) are calculated as follows:

$$de = \bar{\kappa}\, d\bar{p}/\bar{p}\,; \quad (5)$$

$$de = \bar{\lambda}\, d\bar{p}_0/\bar{p}_0 \quad (6)$$

where $\bar{p}$ is the mean effective stress (calculated through Eq. (3)) and $\bar{\kappa}$ the elastic volumetric compressibility assumed constant in this paper, $\bar{p}_0$ is the mean yield stress at the current effective suction and $\bar{\lambda}$ the plastic volumetric compressibility in the void ratio - logarithmic effective stress (Eq. (3)) plane. The structure of $\bar{\lambda}$ will be discussed below.

The effect of non-saturation in the plastic compressibility has been reported by many authors depending on suction and/or degree of saturation. The proposal used in the model presented here is that the unsaturated plastic compressibility, $\bar{\lambda}$, depends on the virgin compressibility index for saturated conditions, $\bar{\lambda}(0)$, and of the current effective suction ($\bar{s}$).

The LC yield function is linked with the volumetric compression index, $\bar{\lambda}$, by the expression:

$$\bar{p}_0/\bar{p}_c = \left(p_0^*/\bar{p}_c\right)^{\frac{\bar{\lambda}(0)-\bar{\kappa}}{\bar{\lambda}(\bar{s})-\bar{\kappa}}} \quad (7)$$

where p_0^* is the preconsolidation isotropic stress for saturated states and $\bar{p}_c$ is a reference mean effective stress corresponding to the point where virgin compression lines cross for different effective suctions. Note that the microstructure does not affect p_0^*. The model assumes that a unique normal saturated consolidation line exists.

The hardening law was made dependent on plastic volumetric strain.

An advantage of using a Bishop-based stress as an effective stress for unsaturated soils (instead of a net stress) is that Terzaghi effective stress is immediately recovered when saturation is reached (S_r=1). However, experimental evidences of the behavior of soils subjected to a suction lower than the air entry value (s_e) indicate that saturated behavior is recovered. It is not automatically reproduced in models defined with a constitutive variable as a function of s or the product $S_r \cdot s$. This drawback can be easily solved by prescribing that the variables depending on suction recover their corresponding saturated values for suctions lower than s_e. The proposal of the model is that the plastic stiffness increase due to non-saturation is linked with the air entry value (s_e). This is done by defining the reduction of $\bar{\lambda}$ by including information taken from the WRC:

$$\bar{\lambda}(\bar{s}) = \lambda(0)\left[\bar{r} + (1-\bar{r})\left[1 - (\bar{s}/\bar{s}_\lambda)^{1/(1-\bar{\beta})}\right]^{-\bar{\beta}}\right] \quad (8)$$

which adopts a form taken from the equation proposed by Van Genuchten for the WRC.

3 MODEL PERFORMANCE

The performance of the model is illustrated for a soil characterized by the model parameters and initial state variables summarized in Table 1. Isotropic loadings tests at constant suction (1MPa) and a subsequent saturation at constant mean net stress (10 MPa) are simulated on samples with different values of e_m (0.1, 0.15, 0.2, 0.25). The initial void ratio is equal to 0.6 for all samples and the initial yield stress at zero effective suction is equal to 0.2 MPa.

A unique set of constitutive parameters describe the "intrinsic" properties of the compacted soils. As-compacted conditions are defined by two initial stress states: suction and (saturated) yield stress. Based on experimental data collected by Romero et al. (2011) [vi] on Boom clay, bentonite and Barcelona silty clay, the selected values of e_m could be appropriate for a low or medium plasticity clay compacted at both dry conditions (low values of e_m) and wet conditions (high values of e_m). A Van Genuchten curve has been selected to represent the water retention features (Table 1).

Table 1. Model parameters used in model performance.

Parameter	*Values*
Mechanical parameters	
$\overline{\kappa}$	0.01 MPa
$\overline{\lambda}(0)$	0.1
$\overline{p}_c$	0.02 MPa
$\overline{s}_\lambda$	0.05 MPa
$\overline{r}$	0.5
$\overline{\beta}$	0.32 MPa^{-1}
n	10
Water retention curve	
$S_{r\min}$	0
$S_{r\max}$	1
P_0	0.05 MPa
λ	0.27

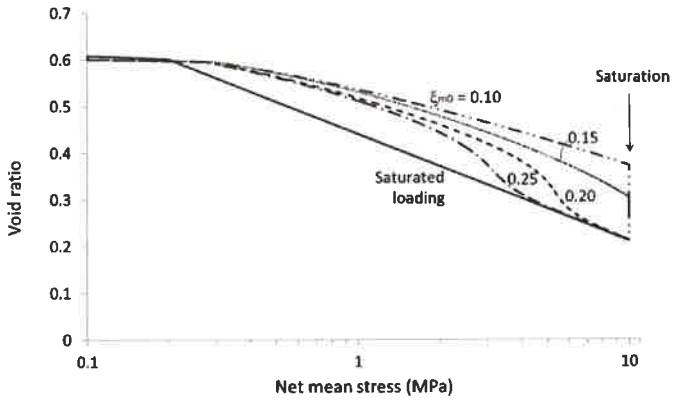

Figure 2. Isotropic loading curves at constant suction (1 MPa) and saturation at 10 MPa of net stress for different values of ξ_{m0}.

Figure 1 shows the computed compression curves. The normal compression line for saturated conditions is also plotted. Compression lines are not linear in the p - s space. At relatively low stress levels, all unsaturated compression curves exhibit a higher stiffness than the saturated compression curve. This is an effect of the current effective suction. As applied stress increases, the curvatures are more pronounced and they converge toward the fully saturated normal consolidation line. This is consequence of the progressive reduction of void ratio during compaction. Since e_m is assumed to remain constant the state variable $\xi_m = e_m / e$ increases continuously and the effective suction, which controls compressibility, decreases.

In the calculated example the WRC is unique and the degree of saturation is maintained during loading. Therefore, the amount of water existing in the sample reduces progressively during loading. Capillary water will eventually disappear (water will remain inside aggregates), the effective suction will reduce to zero and the compressibility will approach the saturated value. Since all samples are subjected to the same suction, samples with higher

values of ξ_{m0} reach the saturated compression lines faster since they have a lower proportion of macropores. Given a microstructure, an initial suction and a WRC, the shape of the compression curves is determined by the shape of the function selected for $\bar{\lambda}(\bar{s})$.

In the simulated cases, samples were saturated when the isotropic net stress reached 10 MPa. The smaller collapse of samples compacted at a higher water content (higher ξ_{m0}) can be observed in Figure 1 (distance between unsaturated and saturated loading curves). Note also that the model is able to reproduce the collapse variation with the applied net stress as observed experimentally ([vii]). The collapse initially increases with the vertical stress, it reaches a maximum value and finally decreases at higher values of net stress.

2 CONCLUSIONS

A constitutive model for compacted soils has been discussed and its capabilities have been illustrated by simulating isotropic loadings.

The model is defined in terms of a Bishop-type constitutive stress and an effective suction. Both constitutive variables include microstructural information. Some relevant conclusions are:

- In the elastic region, successful predictions can be made if a single effective stress, which combines net stress and effective suction, is used.
- Compressibility, defined in terms of logarithmic net stress is a nonlinear function of stress. It is also controlled by the soil microstructure. At high applied stresses the saturated compressibility is recorded in tests. These effects are properly reproduced by the model developed.
- Wetting induced collapse depends on the applied net stress. It increases first at relatively low values of net stress, reaches a maximum and decreases at higher compression values. This is a consequence of the changes in compressibility mentioned before.

REFERENCES

[i] Vaunat, J., E. Romero, C. Jommi, 2000, "An elastoplastic hy-dromechanical model for unsaturated soils". Experimental evidence and theoretical approaches in unsaturated soils (eds A. Tarantino & C. Mancuso). Rotterdam. A. A. Balkema,121:138.

[ii] Alonso, E.E., J.M. Pereira, J. Vaunat, S. Olivella, 2010, "A microstructurally based effective stress for unsaturated soils". Géotechnique 60(12), 913:925.

[iii] Della Vecchia G., C. Jommi , E. Romero, 2012, "A fully coupled elastic-plastic hydro-mechanical model for compacted soils accounting for clay activity". Int. J. Num. An. Met. in Geomech 37 (5), 503:535.

[iv] Delage P., G. Lefebvre, 1984, "Study of the structure of a sensitive Champlain clay and of its evolution during consolidation". Canadian Geotechnical Jnl. 21(1), 21:35

[v] Alonso, E.E., A. Gens, A. Josa, 1990. "A constitutive model for partially saturated soils". Géotechnique 40 (3). 405:430

[vi] Romero, E., G. Della Vecchia, C. Jommi, 2011, "An insight into the water retention properties of compacted clayey soils". Géotechnique 61(4), 313:328.

[vii] Suriol, J. A. Lloret, 2007 "Cambios en la estructura de suelos compactados frente a humedecimiento y secado". Ingeniería Civil, Madrid, 147, 67:76